



 Cite this: *RSC Adv.*, 2026, 16, 26928

# Active food packaging based on chitosan–lignin with encapsulated argan oil for meat shelf-life extension

 Abdellah Halloub<sup>a</sup> and Marya Raji \*<sup>b</sup>

In recent years, the demand for sustainable and functional food packaging derived from bio-based resources has increased significantly. This study reports the development of an active bio-based film with antioxidants, antibacterial, and UV-shielding properties, based on chitosan and lignin, aimed at extending the shelf life of meat products. The film incorporates argan oil microcapsules, in which argan oil is encapsulated within an alginate shell and dispersed in a chitosan–lignin matrix. The structural, thermal, and functional properties of the films were characterized using thermogravimetric analysis (TGA), Fourier transform infrared spectroscopy (FT-IR), scanning electron microscopy (SEM), and UV-visible spectroscopy. The incorporation of argan oil microcapsules significantly improved antioxidant activity, with DPPH radical scavenging increasing from 48.3% to 64.6%. In addition, the films exhibited antimicrobial potential, extending the shelf life of meat by approximately one additional day compared with control films without microcapsules. A preliminary application test using ground meat showed improved visual color stability when packaged with the microcapsule-containing film compared with the control film during short-term storage. They also show an increased elongation at break, more than doubling from  $16.03 \pm 1.70\%$  to  $34.97 \pm 2.85\%$ , confirming that the presence of microcapsules improved film flexibility by facilitating plastic deformation. Moreover, the films demonstrated excellent UV-blocking capability, with absorbance values close to 4.0 A.U. across the UV region (200–570 nm), indicating that the UV-barrier properties were largely preserved after microcapsule incorporation. These results highlight the strong potential of chitosan–lignin films containing argan oil microcapsules as sustainable active packaging materials for protecting perishable foods and extending shelf life.

 Received 30th October 2025  
 Accepted 6th April 2026

DOI: 10.1039/d5ra08351f

[rsc.li/rsc-advances](http://rsc.li/rsc-advances)

## Introduction

The escalating global concern about food loss and waste highlights the urgent need for innovative and effective strategies to improve food preservation. According to global food waste estimates approximately 1.3 billion tons of food intended for human consumption are lost or wasted each year, demonstrating the scale of this global challenge. Effective food packaging systems can potentially reduce 20–25% of this loss by extending the shelf life of food products and preventing microbial growth responsible for spoilage and foodborne illnesses.<sup>1</sup> According to the World Health Organization (WHO), foodborne diseases caused approximately 420 000 deaths in 2010, emphasizing the importance of developing safe and sustainable food preservation technologies.<sup>2,3</sup>

Food spoilage is mainly caused by enzymatic reactions, microbial contamination, and oxidative degradation, all of which negatively affect food quality and safety.<sup>4</sup> Although synthetic preservatives have traditionally been used to control these processes, increasing health and environmental concerns have led to a growing demand for natural and sustainable preservation strategies.<sup>5</sup> In this context, natural antioxidants such as essential oils, polyphenols, and plant extracts have attracted considerable attention due to their ability to inhibit lipid oxidation and microbial growth while maintaining food quality.<sup>6,7</sup>

Despite their promising bioactivity, the direct incorporation of essential oils or plant-derived bioactive compounds into polymer matrices often presents significant limitations. These compounds are typically volatile, sensitive to heat, oxygen, and light, and may rapidly degrade or evaporate, which reduces their effectiveness during food storage.<sup>8</sup> Furthermore, their strong aroma and rapid release from packaging matrices can limit their practical application in food packaging systems. To overcome these limitations, microencapsulation techniques have been widely explored to enhance the stability and controlled release of bioactive compounds. Encapsulation systems can protect sensitive molecules from environmental

<sup>a</sup>Faculty of Chemistry, Nicolaus Copernicus University in Toruń, 7 Gagarina Street, Toruń 87-100, Poland

<sup>b</sup>College of Chemical Sciences and Engineering (CCSE), Department of Materials Science, Energy and Nano-engineering (MSN), Mohammed VI Polytechnic University (UM6P), 43150 Benguerir, Morocco. E-mail: maria.raji@um6p.ma


degradation while allowing their gradual release over time. Various encapsulation approaches, including liposomes, polymeric particles, and solid lipid nanoparticles, have demonstrated significant potential for stabilizing natural oils and preserving their antioxidant and antimicrobial properties.<sup>9</sup>

Biopolymer-based films have emerged as promising materials for sustainable active food packaging, particularly when combined with functional natural additives. Among these materials, chitosan is widely recognized for its excellent film-forming ability, biodegradability, and inherent antimicrobial activity.<sup>10</sup> Lignin, a natural aromatic biopolymer, provides strong UV-shielding and antioxidant properties due to its phenolic structure, making it particularly attractive for food packaging applications.<sup>11,12</sup> In addition, the use of gum Arabic as a stabilizing and emulsifying agent during microcapsule formation improves emulsion stability and facilitates the formation of a protective wall around oil droplets. Furthermore, alginate is commonly used as an encapsulating agent because of its biocompatibility, film-forming capability, and ability to form stable microcapsule shells that protect bioactive compounds and control their release.<sup>13</sup> Among natural bioactive oils, argan oil, extracted from the kernels of *Argania spinosa*, has gained considerable interest due to its high nutritional and bioactive value. *Argania spinosa*, native to southwestern Morocco, represents an important natural resource with significant potential for food and packaging applications.<sup>14,15</sup> Argan oil is rich in tocopherols (60–90 mg/100 g), sterols (<220 mg/100 g), mono-unsaturated fatty acids (43–49.1%), and polyunsaturated fatty acids (29–36.3%), which contribute to its strong antioxidant and antimicrobial properties.<sup>16–18</sup> Previous studies have demonstrated that argan oil can inhibit the growth of foodborne pathogens such as *Staphylococcus aureus* and *Escherichia coli*, mainly due to the presence of phenolic compounds and tocopherols that disrupt bacterial cell membranes.<sup>19,20</sup> In addition to argan oil, lignin derived from argan nutshells (ANS) represents a valuable by-product of argan oil production and offers additional functionality for food packaging materials. This lignin contains phenolic structures capable of absorbing UV radiation and scavenging free radicals, making it particularly suitable for developing multifunctional active packaging films.<sup>12</sup>

To the best of our knowledge, this is the first study combining argan-shell-derived lignin and alginate-encapsulated argan oil within a chitosan-based active packaging film for meat preservation applications. The objective of this study was to develop UV-protective and antioxidant biofilms by encapsulating argan oil within alginate microcapsules using gum Arabic as a stabilizing and emulsifying agent, then incorporating these microcapsules into a chitosan–lignin film matrix. The developed films were evaluated in terms of their structural, thermal, antioxidant, antimicrobial, and UV-shielding properties, as well as their effectiveness as active packaging materials for extending the shelf life of meat products.

## Materials and methods

### Materials

Argan nutshells (ANS) were collected as by-products of argan fruit processing in rural regions of southwestern Morocco.

Argan oil and gum Arabic were purchased from a local Moroccan drugstore in food-grade quality. Fresh ground beef (80% lean) was obtained from a local butcher shop in Rabat, Morocco. Sodium alginate (CAS 9005-38-3, M/G ratio = 0.6) and chitosan (CAS 9012-76-4, degree of deacetylation = 85%) were purchased from Sigma-Aldrich and used as received. Calcium chloride, sodium hydroxide, and acetic acid were also obtained from Sigma-Aldrich and were of analytical grade. All materials were used without further purification unless otherwise specified.

### Lignin extraction

Lignin was extracted from argan nutshells following the procedure previously reported in our work.<sup>21</sup> Briefly, ANS particles were mixed with a 6.4% (w/v) sodium hydroxide (NaOH) solution and magnetically stirred for 4 h at 80 °C to solubilize the lignin fraction. The resulting mixture was filtered to separate the solid residues from the black liquor. Subsequently, acetic acid was gradually added to the filtrate until the pH reached 6–7, inducing lignin precipitation. The precipitated lignin was collected, washed several times with distilled water to remove residual chemicals, and stored at 4 °C until further use.

### Microcapsule preparation

Argan oil microcapsules were prepared using an oil–water–oil (O/W/O) emulsification method, following the procedure described in our previous study.<sup>22</sup> In this system, argan oil acted as the core material, while alginate served as the primary shell material with a core-to-shell ratio of 70 : 30 (w/w). First, 50 mL of distilled water was mixed with 0.4 g of sodium alginate and 0.1 g of gum Arabic, and the solution was magnetically stirred at 400 rpm and 25 °C until complete dissolution. Subsequently, 1.16 g of argan oil was added to the solution, and the mixture was stirred at 500 rpm and 25 °C until a stable primary emulsion was obtained (emulsion A). The resulting emulsion A (~51 mL) was then added dropwise using a syringe into 300 mL of vegetable oil under magnetic stirring (500 rpm, 25 °C) over 15 min to form the O/W/O system. After emulsification, 150 mL of calcium chloride solution (4 wt%) was added to induce ionic crosslinking of the alginate shell and stabilize the formed microcapsules. The system was left undisturbed for 24 h, after which the microcapsules accumulated at the interface between the aqueous and oil phases. The microcapsules were collected by filtration and washed with ethanol to remove residual oil. The purified microcapsules were then stored at 4 °C until further use. Fig. 1 illustrates the microcapsule preparation procedure.

### Film preparation

The films were manufactured *via* the solvent-casting method using a biopolymer matrix comprising 40 wt% chitosan and 50 wt% lignin, 9 wt% microcapsules, and 1 wt% glycerol. Based on preliminary optimization trials, a microcapsule concentration of 9 wt% was selected to balance functional performance and structural integrity. Lower concentrations (5 wt%) resulted in reduced antioxidants and UV-blocking efficiency, whereas



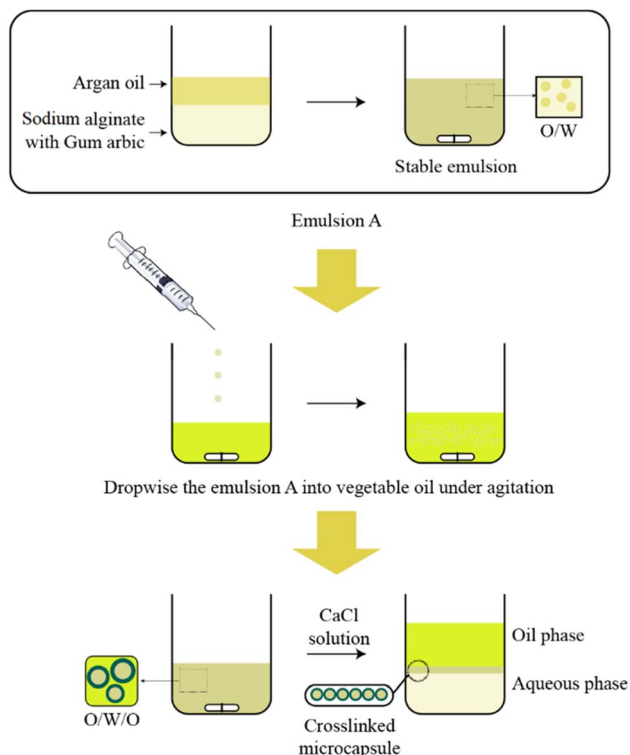


Fig. 1 Argan oil microcapsule manufacturing.

higher concentrations (15 wt%) compromised the mechanical properties and homogeneity of the film matrix. This concentration aligns with findings from similar studies, which

Table 1 Chemical composition of films

Films	Code	Composition
Film without microcapsules	WOM	Lignin 49 wt% Chitosan 50 wt% Glycerol 1 wt%
Film with microcapsules	WM	Lignin 40 wt% Chitosan 50 wt% Microcapsules 9 wt% Glycerol 1 wt%

demonstrate the effectiveness of comparable additive levels in biopolymer-based films for active food packaging applications. Additionally, a reference film was made with 40 wt% chitosan, 59 wt% lignin, and 1 wt% glycerol to study the effect of the absence of microcapsules. The film preparation process started by dissolving 0.4 g of chitosan in 40 mL of diluted acetic acid solution and magnetically stirring at 25 °C for 24 hours to obtain a homogenized solution. Subsequently, 0.5 g of lignin was added to the chitosan solution, along with 0.01 g of glycerol. The mixture was then magnetically stirred for 4 hours. Next, 0.09 g of microcapsules was added to the mixture, and the mixture was stirred for an additional 2 hours at room temperature. The film-forming solution was poured into 90 mm plastic Petri dishes and dried under ambient conditions ( $22 \pm 2$  °C, ~50% RH) for 48 hours. After drying, the films were carefully peeled off and stored in sealed containers at room temperature before further analysis, see Fig. 2. The same film preparation process was applied to create the reference film without the

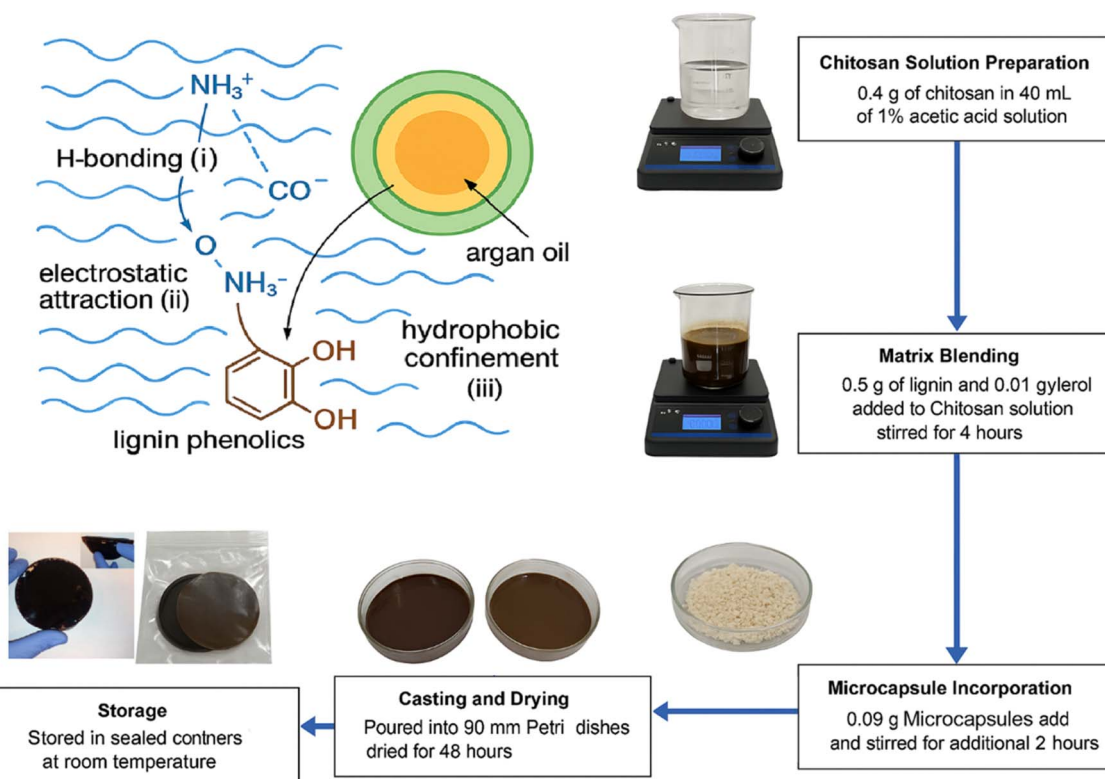


Fig. 2 Film preparation with microcapsules.



microcapsules. The detailed compositions of the prepared films are summarized in Table 1.

## Characterizations

### Fourier transform infrared (FTIR) spectroscopy

The Fourier transforms infrared (FTIR) spectra of the microcapsules, argan oil, lignin, chitosan, Ca-alginate, and films were recorded *via* a PerkinElmer two Fourier transform infrared spectrometer in attenuated total reflectance (ATR) mode with a diamond crystal. The measurements were performed with a spectral resolution of  $4\text{ cm}^{-1}$  with 8 scans per spectrum in the region of  $4000\text{--}500\text{ cm}^{-1}$ .

### Thermogravimetric analysis (TGA)

Thermogravimetric analysis (TGA) of each compound was conducted *via* a Q500 instrument from TA Instruments. A representative sample (10–20 mg) of each compound was placed in a platinum pan. The analysis was performed under a nitrogen gas atmosphere with a flow rate of  $40\text{ mL min}^{-1}$ . The heating process started at ambient temperature and continued up to  $800\text{ }^\circ\text{C}$ , with a heating rate of  $10\text{ }^\circ\text{C min}^{-1}$ . This analysis allowed the examination of the thermal properties of the compounds and their behavior under increasing temperature conditions.

Encapsulation metrics were determined by thermogravimetric analysis (TGA). The residual mass fraction at  $600\text{ }^\circ\text{C}$  (under  $\text{N}_2$ , at a heating rate of  $10\text{ }^\circ\text{C min}^{-1}$ ) was measured for three replicates each of: (i) pure argan oil (core material), (ii) the pure shell material, and (iii) the final microcapsules. Denoting the mean residual fractions as  $R_{\text{core}}$ ,  $R_{\text{shell}}$ , and  $R_{\text{caps}}$ , respectively, the core mass fraction ( $f_{\text{core}}$ ) was calculated using a high-temperature mass balance, using eqn (1)–(3).<sup>23</sup>

$$R_{\text{caps}} = f_{\text{shell}} \times R_{\text{shell}} + f_{\text{core}} \times R_{\text{core}} \quad (1)$$

$$f_{\text{shell}} + f_{\text{core}} = 1 \quad (2)$$

Solving for  $f_{\text{core}}$  yields:

$$f_{\text{core}} = \frac{R_{\text{caps}} - R_{\text{shell}}}{R_{\text{core}} - R_{\text{shell}}} \quad (3)$$

Given that edible oils like argan oil are nearly fully volatile under these conditions ( $R_{\text{core}}$ ), the equations simplify to eqn (4).<sup>23</sup>

$$f_{\text{shell}} = 1 - R_{\text{caps}}/R_{\text{shell}} \quad (4)$$

The loading capacity (LC%) and encapsulation efficiency (EE%) were then calculated using eqn (5) and (6).<sup>23</sup>

$$\text{LC}\% = 100 \times f_{\text{core}} \quad (5)$$

$$\text{EE}\% = 100 \times \frac{f_{\text{core}}}{f_{\text{core theoretical}}} \quad (6)$$

where  $f_{\text{core theoretical}}$  is the target oil mass fraction based on the initial feed recipe. All reported values are presented as mean  $\pm$  standard deviation (SD).

### Scanning electron microscopy (SEM)

Scanning electron microscopy (SEM) is an important technology used to explore the size and shape of microcapsules, as well as their dispersion in films. In this study, SEM analysis was conducted *via* a scanning electron microscope (HIROX SH 4000 M) at a voltage of 15 kV. Before analysis, all the samples were coated with a thin layer of conductive carbon *via* an ion-sputtering device. This coating process enhances the conductivity of the samples and ensures high-quality imaging during SEM analysis. By employing SEM, researchers can visualize and characterize the morphology and distribution of the microcapsules within the film, providing valuable insights into their structural properties. To further examine the interior design of the microcapsules, an extraction process was carried out using acetone to release the encapsulated argan oil.

### Tensile testing

Following ISO 527-1:2012.17, tensile tests for the film were conducted *via* a Tinius Olsen H10KT universal testing machine. The tests were performed with a crosshead speed of  $3\text{ mm min}^{-1}$  and a 1 kN load cell. Specimens measured  $80\text{ mm} \times 10\text{ mm} \times$  film thickness  $\sim 0.1\text{ mm}$ . The film's stress–strain curves were obtained during the tensile tests. Young's modulus, tensile strength, elongation at break, toughness, and strain at yield were among the tensile characteristics calculated *via* the film's stress–strain curves. Each test was performed in triplicate for each film formulation to ensure statistical reliability.

### Water swelling properties

The WM (with microcapsules) and WOM (without microcapsules) films, each measuring  $20 \times 10\text{ mm}$ , were immersed in water with a pH value of 7.23. Gravimetric measurements were conducted at different time intervals to determine the films' weights while they were in contact with water. The percentages of weight increase were then calculated based on the changes in weight over time. Each measurement was performed in triplicate.

Before weighing, the film samples were blotted with blotting paper to remove any excess surface water. This step ensured that only the water absorbed into the film was measured, and any excess water on the surface was excluded from the calculations. By monitoring weight gain over time, researchers can evaluate the water absorption and water retention properties of films, which are important factors in understanding their behavior under moist conditions or potential applications involving contact with liquids.

### DPPH antioxidant activity

The DPPH (2,2-diphenyl-1-picrylhydrazyl) free radical scavenging assay was used to assess the antioxidant properties of the films. Each film, weighing approximately 20 mg, was immersed in 10 mL of methanol and kept in the dark at room temperature for 24 hours. All tests were performed in three independent replicates. Afterward, 2 mL of the film extract solution was combined with 1 mL of a 0.1 mM DPPH methanol



solution. The mixture was vigorously shaken and incubated in the dark for 30 minutes. Finally, a UV-vis spectrophotometer was used to measure the absorbance of the solution at 517 nm, and the DPPH scavenging activity (DPPH%) was calculated as follows by eqn (7):<sup>24</sup>

$$\text{DPPH}(\%) = \frac{A_0 - A}{A_0} \times 100 \quad (7)$$

Here,  $A_0$  represents the absorbance value of the control extracts, whereas  $A$  represents the absorbance value of the sample extracts.

### UV shielding

The optical properties of the films, with and without microcapsules, were analyzed *via* a Varian Cary 300 UV-vis spectrometer, which operates within the wavelength range of 200–800 nm.

### Antibacterial properties

The antibacterial activity of the films was evaluated against *Staphylococcus aureus* (ATCC-6538), *Pseudomonas aeruginosa* (ATCC-9027), and *Escherichia coli* (ATCC-8739), using an agar contact assay based on a modified protocol of ISO 22196. Each bacterial strain was cultured overnight in nutrient broth at 37 °C, and the suspensions were adjusted to approximately 10<sup>8</sup> CFU mL<sup>-1</sup>. Agar plates were inoculated with the bacterial suspension, and sterile film samples (1 cm<sup>2</sup>) of chitosan–lignin films with microcapsules (WM) and without microcapsules (WOM) were placed on the agar surface. After incubation at 37 °C for 24 h, antibacterial activity was evaluated by observing bacterial growth under and around the films. Because antimicrobial compounds incorporated into polymer matrices often act through contact-based mechanisms with limited diffusion, inhibition was mainly assessed at the film–bacteria interface rather than by measuring inhibition halos. All experiments were performed in duplicate and repeated twice to ensure reproducibility. This assay provides qualitative evidence of antibacterial potential, while quantitative microbiological analyses will be required in future studies to more rigorously evaluate the effectiveness of the films in extending the shelf life of meat products.

### Packaging ability

To investigate the antioxidant behavior of the film on food, ground meat was utilized to evaluate the ability of the microcapsule-based film to extend the shelf life of the food product. A 30 g sample of prepared ground meat was placed in a plastic dish at room temperature, and two different samples were prepared: one sample was covered with the film without the microcapsules, and the other sample was covered with the film containing the microcapsules (as shown in Fig. 3). Both samples were placed in direct contact with the films in plastic dishes. While room temperature ( $\approx 25$  °C) was used, commercial storage is typically under refrigeration; this should be considered in future studies. The samples were monitored for 72 h for visual changes and oxidative spoilage. Future studies

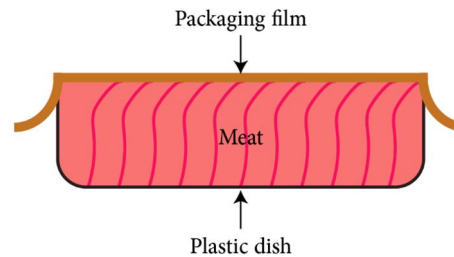


Fig. 3 Grounded meat packaging setup.

will also include a treatment in which the essential oil is added to the packaging in a non-encapsulated form to distinguish encapsulation effects from simple incorporation of the oil. Color determination of ground meat during storage, the CIE-LAB (Commission internationale de l'éclairage,  $L^*$ ,  $a^*$ , and  $b^*$ ) color space was used to provide  $L^*$ ,  $a^*$ , and  $b^*$  values. Where  $L^*$  is lightness from  $L = 0$  for black to  $L = 100$  for white,  $a^*$  is the degree of redness or greenness from  $a^* = -60$  for green to  $a^* = 60$  for red, and  $b^*$  is the degree of yellowness or blueness from  $b^* = -60$  for blue to  $b^* = 60$  for yellow.

### Statistical analysis

All measurements were performed in triplicate using independent film batches. Data were analyzed using one-way ANOVA. Since only two treatments were compared, additional post-hoc tests were not necessary. Results are expressed as mean  $\pm$  SD ( $p \leq 0.05$ ).

### Sampling and randomization

Experiments were conducted using independently prepared batches. Coded sample labels were prepared, shuffled, and randomly drawn by an assistant blind to the samples. Subsamples for tensile tests were taken from spatially distinct regions, and antibacterial assays were arranged according to a randomized grid. All randomization sequences were recorded to ensure transparency.

## Results and discussion

### Fourier transform infrared (FTIR) spectroscopy

FTIR characterization was performed on alginate, argan oil, chitosan, lignin, microcapsules, lignin–chitosan film without microcapsules (WOM), and lignin–chitosan film with microcapsules (WM), as depicted in Fig. 4. The FTIR spectra of alginate, argan oil, and microcapsules are presented in Fig. 4a. In the FTIR spectrum of alginate, several characteristic peaks were observed: O–H stretching at 3273 cm<sup>-1</sup>, aliphatic C–H stretching at 2926 cm<sup>-1</sup>, asymmetric and symmetric COO<sup>-</sup> stretching at 1585 cm<sup>-1</sup> and 1410 cm<sup>-1</sup>, respectively, C–O stretching at 1298 cm<sup>-1</sup>, and C–O/C–C stretching at 1081 cm<sup>-1</sup>. These observations are consistent with previously reported alginate spectra.<sup>25,26</sup> Argan oil exhibits typical bands at 2923 and 2853 cm<sup>-1</sup> (CH<sub>2</sub> stretching), 1744 cm<sup>-1</sup> (C=O stretching), and other characteristic peaks at 1462, 1378, 1237, 1160, 1119, 1097,



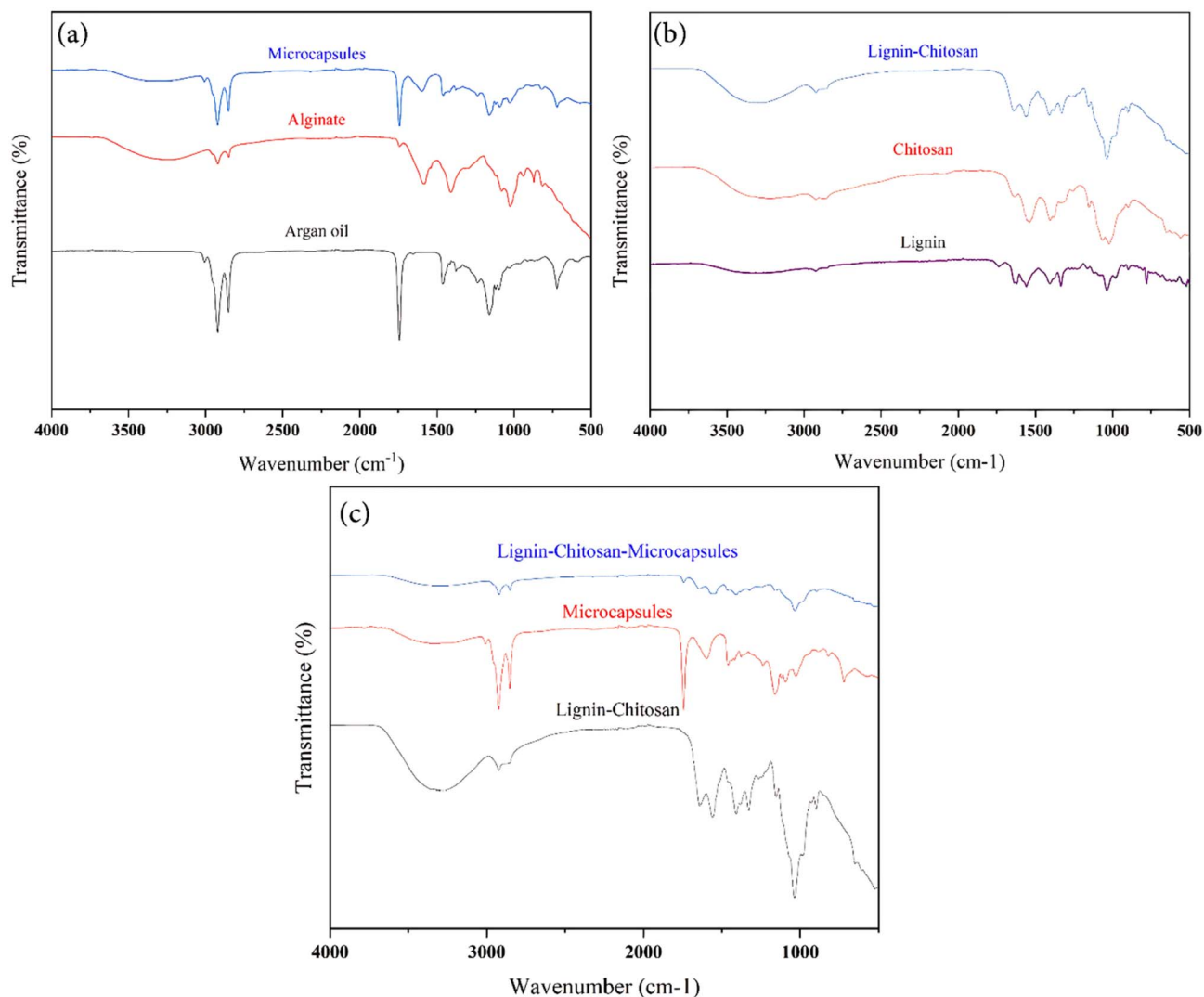


Fig. 4 FTIR spectra of (a) the microcapsules and their compounds, (b) the lignin–chitosan film and its compounds, and (c) the lignin–chitosan–microcapsule film and its compounds.

and 722 cm<sup>-1</sup>, in agreement with the literature.<sup>27,28</sup> In the spectrum of the microcapsules, all major bands of argan oil were preserved, with no significant shifts, suggesting that the encapsulation process did not chemically modify the oil. Small shifts were observed in alginate peaks within the microcapsules (3273 to 3315 cm<sup>-1</sup>; 1585 to 1600 cm<sup>-1</sup>; 1081 to 1092 cm<sup>-1</sup>), which can be attributed to hydrogen bonding and weak electrostatic interactions between alginate and gum Arabic.<sup>29,30</sup>

The lignin, chitosan, and lignin–chitosan composite films (Fig. 4b) exhibit characteristic peaks of both polymers. Chitosan shows broad O–H/N–H stretching (3244–3350 cm<sup>-1</sup>), C–H stretching (2923, 2860 cm<sup>-1</sup>), amide I/II/III peaks (1635, 1542, 1335 cm<sup>-1</sup>), and C–O stretching (1064, 1020 cm<sup>-1</sup>) 28–30. Lignin presents hydroxyl groups (3305 cm<sup>-1</sup>), C–H stretching (2926, 2850 cm<sup>-1</sup>), carbonyl stretching (1740 cm<sup>-1</sup>), and aromatic skeletal vibrations (1625, 1560, 1406 cm<sup>-1</sup>).<sup>21,31</sup> Upon blending, FTIR spectra reveal peak shifts (e.g., amide I 1635 to 1642 cm<sup>-1</sup>, amide II 1542 to 1562 cm<sup>-1</sup>), confirming hydrogen

bonding between lignin and chitosan.<sup>32,33</sup> In the WM film, microcapsule incorporation does not significantly alter the main film peaks, except for the argan oil C=O peak at 1745 cm<sup>-1</sup>, confirming successful incorporation without structural alteration of the matrix. Comparison with similar studies shows consistent results, e.g., microencapsulation of essential oils in biopolymer matrices often preserves core chemical integrity while inducing minor shell shifts.<sup>34</sup>

### Thermogravimetric analysis (TGA)

The thermal stabilities of microcapsules, WM, and WOM films, as well as their constituent materials, were investigated to determine their temperature limits for use in thermosealing food packaging applications. The results are presented in Fig. 5, where TGA and DTG thermograms of the argan oil, alginate, and argan oil-based microcapsules are displayed. According to the TGA curve of pure argan oil, thermal degradation occurs in a single-step triglyceride degradation (310–465 °C), with the



maximum degradation temperature observed at 419 °C.<sup>35</sup> In contrast, sodium alginate undergoes a two-step degradation: the first between 200–220 °C ( $T_{\max} \approx 210$  °C) and the second between 220–290 °C ( $T_{\max} \approx 260$  °C), corresponding respectively to dehydration and cleavage of glycosidic bonds, followed by decarboxylation and formation of CaO/Ca(OH)<sub>2</sub> residues. A final minor event occurs at 650–750 °C ( $T_{\max} \approx 735$  °C), consistent with the oxidative decomposition of the remaining carbonaceous char. The DTG curve shown in Fig. 5b for the microcapsules reveals a multistep thermal degradation profile composed of four distinct stages. The first degradation band (i), observed between 180 and 220 °C, corresponds to the initial scission of the alginate backbone, indicating the onset of polymer decomposition. In the same temperature region, a broader degradation event extending from 215 to 320 °C, with a DTG maximum around 258 °C, is attributed to the primary decomposition of the alginate shell matrix, which involves depolymerization and the breakdown of glycosidic linkages in the polysaccharide network.<sup>36</sup> The second band (ii) appears between 330 and 400 °C, with a maximum mass-loss rate of –5.9% per min at approximately 370 °C. This stage is mainly

associated with the release and volatilization of the encapsulated argan oil, facilitated by structural changes in the polymeric shell during heating. The microcapsule architecture produced through the oil-in-water (o/w) emulsion process disperses the oil as fine droplets within the biopolymer matrix, increasing the interfacial surface area and promoting mass transfer during thermal treatment. Consequently, once the shell structure begins to deteriorate, the encapsulated oil can volatilize more readily than in the bulk state. While emulsification may slow oxidation due to physical barriers created by surfactants and small droplets, the presence of water and interfacial reactions can also promote hydrolysis or pro-oxidant processes during heating.<sup>37,38</sup> At higher temperatures, alginate undergoes secondary degradation (iii) between 420 and 525 °C, corresponding to the decomposition of residual carbonaceous structures and further breakdown of the polysaccharide matrix. Finally, band (iv), observed as a minor endothermic signal around 625 °C, is attributed to inorganic residues such as NaCl, originating from the ionic crosslinking process used during microcapsule formation.<sup>39</sup> The char yield of the microcapsules at 600 °C ( $R_{\text{caps}} = 17.0\%$ ) lies between that of pure alginate

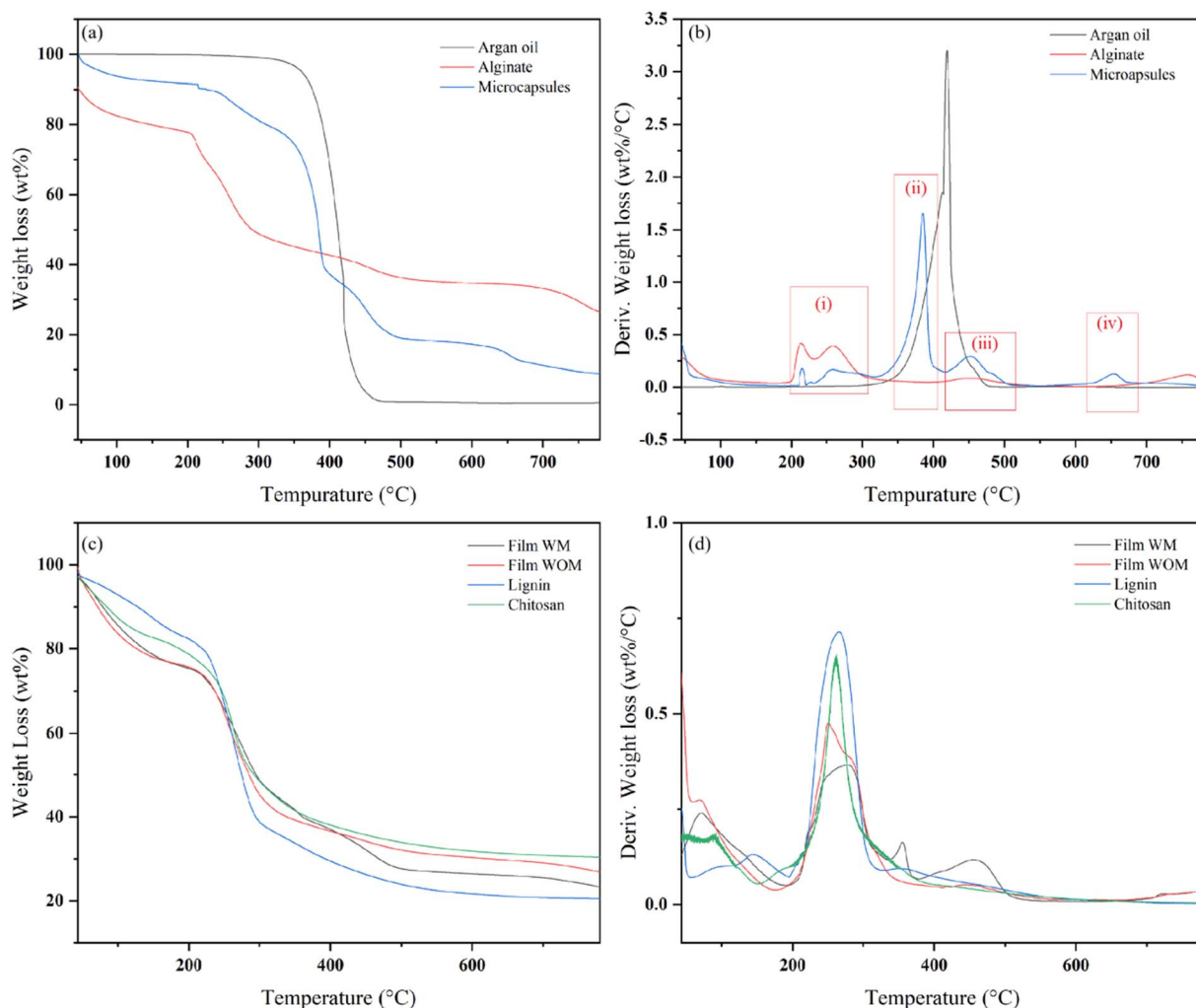


Fig. 5 TGA and DTG curves of (a and b) microcapsules and their materials and (c and d) films and their materials.



( $R_{\text{shell}} = 34.6\%$ ) and pure argan oil ( $R_{\text{core}} = 0\%$ ), confirming partial encapsulation of the oil phase. From this residue balance, the loading capacity ( $LC = 50.9\%$ ) and encapsulation efficiency ( $EE = 72.7\%$ ) were calculated, evidencing efficient core-shell formation and stable microcapsule architecture.<sup>40,41</sup> The encapsulation efficiency of the microcapsules can be estimated from the 600 °C char residue because alginate and argan oil behave very differently at this temperature. At this temperature, pure alginate  $R_{\text{shell}}$  still retains 34.6% of its original mass, whereas pure argan oil leaves no residue at all ( $R_{\text{core}} = 0$ ). Indeed, the residue of microcapsules at 600 °C was 17.0%. The calculated loading capacity (LC) was  $LC = 50.9\%$ . Subsequently, the encapsulation efficiency (EE) was calculated relative to the theoretical loading target of 70%, resulting in 72.7%. Finally, for films with 9 wt% capsules, the actual oil content was approximately 4.6 wt%. On the other hand, thermogravimetric analysis (TGA) and derivative thermogravimetry (DTG) of lignin, chitosan, WOM film (chitosan-lignin without microcapsules), and WM film (with alginate encapsulated argan oil) are shown in Fig. 5c and d. The initial weight loss observed below 160 °C in all samples is attributed to the evaporation of physically adsorbed and bound water. Pure chitosan displayed a single major degradation step with a DTG peak at 306.4 °C. Lignin showed a broader, multi-stage degradation profile: an initial event near 202 °C largely associated with pyrolysis of guaiacyl/syringyl structures, followed by a gradual decomposition above ~322 °C (*p*-coumaryl and syringyl-rich domains), leaving around 20% residue at 780 °C, indicative of condensed aromatic char formation.<sup>42</sup> When chitosan was blended with lignin (WOM film), the principal chitosan degradation peak shifted downward to 261.7 °C, suggesting that lignin-chitosan interactions (and the associated disruption of chitosan-chitosan hydrogen bonding) facilitate earlier thermal scission in the matrix.<sup>43</sup> The higher-temperature lignin degradation region was

largely retained, so the overall char yield remained high. Incorporation of microcapsules (WM film) did not substantially alter the early moisture loss region of the matrix but introduced two additional DTG signals: a first peak between 320–404 °C (max ~355 °C) attributed to decomposition of the alginate microcapsule wall, and a second peak between 410–505 °C (max ~454 °C) associated with the thermal degradation/volatilization of encapsulated argan oil. The high-temperature residue of the WM film was slightly greater than that of WOM, consistent with mineral content from the alginate phase and the inherent char-forming tendency of lignin. Indeed, adding microcapsules broadens the multi-step degradation but does not compromise the low-temperature stability window relevant to film casting or refrigerated food storage. Operational temperatures for meat packaging (<10 °C storage; <60–80 °C processing) remain well below the onset of major thermal decomposition for either film type.

### Scanning electron microscopy (SEM)

The morphological properties of the microcapsules and the films were analyzed by scanning electron microscopy (SEM). Fig. 6 presents SEM images of the microcapsules and fractured sections of the films, both with and without microcapsules. From the SEM micrographs, it is evident that the dried microcapsules display irregular shapes and surfaces with bumps. This can be attributed to the evaporation and shrinkage of water within the calcium alginate shell during the drying process. Moreover, the multicore argan oil (AO) remained intact within the microcapsules, resulting in bumpy surfaces that corresponded to the shape of the encapsulated multicore. This confirmed the successful encapsulation of argan oil within microcapsules. To further examine the interior design of the microcapsules, an extraction process was used; the SEM

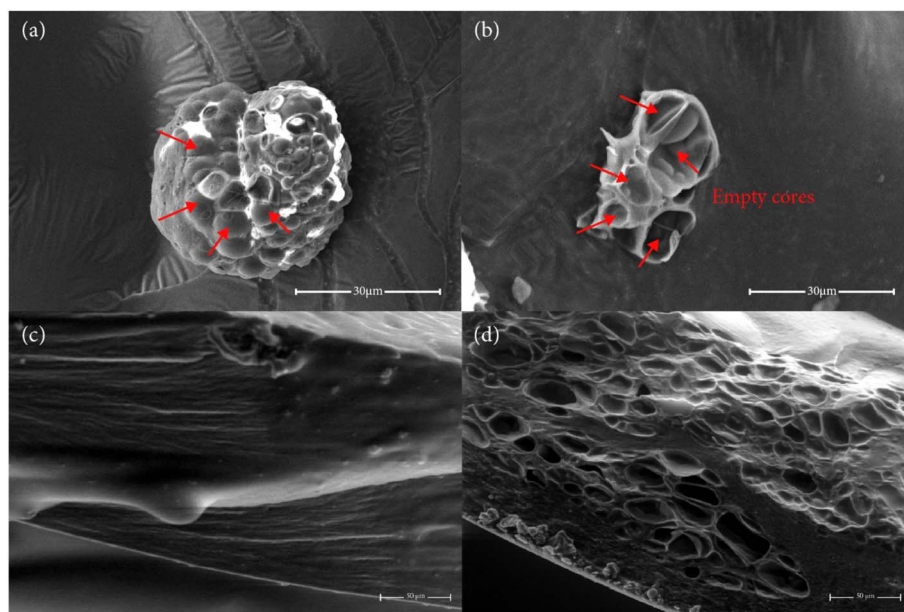


Fig. 6 SEM micrographs of (a and b) the AO microcapsule and cracked microcapsule, and (c and d) film WOM and WM cross-sections.



micrograph revealed a porous interior structure within the microcapsules, with a size of the chambers ranged from 3 to 14  $\mu\text{m}$ . This porous structure is attributed to the presence of the capsule cores, which are occupied by the argan oil.<sup>44</sup> Similar morphologies appeared in the work by Soliman *et al.*<sup>45</sup> in which alginate microspheres with many essential oils (EOs), such as garlic, cinnamon, thyme, oregano, clove, basil, coriander, citrus peel, eucalyptus, ginger, rosemary, and peppermint. In their work, SEM images showed three-dimensional porous bead structures resembling a sponge-like network composed of cavities and surrounding walls. This morphology corresponds to the well-known “egg-box” structure of alginate, confirming the entrapment of essential oils within the cavities of the alginate matrix. The multicore argan oil calcium alginate microcapsules developed in this work were produced *via* an emulsion-drying method and subsequently incorporated into chitosan-lignin films. Compared with other encapsulation approaches, such as electrospraying,<sup>46</sup> extrusion,<sup>47</sup> or microfluidic techniques,<sup>48</sup> the present system generates smaller internal chambers (3–14  $\mu\text{m}$ ) while preserving the integrity of the multicore oil droplets after drying. The surface bumps observed on the microcapsules indicate that the oil cores remain intact despite shell shrinkage, resulting in a well-defined porous internal structure rather than a homogeneous sponge-like network.

SEM micrographs of the fractured cross-sections of the films, shown in Fig. 6c and d, reveal that the film without microcapsules exhibits a smooth and uniform morphology. This smooth surface indicates good miscibility between the chitosan and lignin biopolymers, leading to the formation of a homogeneous film structure. In contrast, the microcapsule-containing film displays several oval-shaped cavities of various sizes in its cross-section. These cavities are mainly attributed to microcapsule rupture during sample preparation for SEM analysis. Despite the presence of these cavities, the microcapsules exhibit good adhesion to the film matrix, suggesting strong interactions between the alginate shell and the chitosan-lignin polymer network. SEM measurements also revealed that the average thickness of the film without microcapsules (WOM) was  $181.4 \pm 3.3 \mu\text{m}$ , whereas the film containing microcapsules (WM) exhibited a slightly higher thickness of  $195.9 \pm 2.8 \mu\text{m}$ . This increase in thickness is consistent with the incorporation of discrete microcapsular structures within the polymer matrix, which slightly increases the overall film thickness.

### Tensile testing

The mechanical performance of the chitosan-lignin films was analyzed to evaluate the influence of argan oil microcapsules on the tensile behavior of the biopolymer matrix. Representative stress-strain curves for films with (WM) and without (WOM) microcapsules are shown in Fig. 7. The incorporation of alginate microcapsules produced a pronounced effect on the films' mechanical response, transforming their behavior from brittle to more ductile. Quantitatively, the Young's modulus of the WM film in Fig. 7b decreased significantly by approximately 85.8%, from  $232.98 \pm 5.67 \text{ MPa}$  (WOM) to  $33.14 \pm 2.80 \text{ MPa}$  ( $p = 6.7 \times 10^{-7}$ ). This result indicates a highly significant reduction in

stiffness caused by microcapsule incorporation, which serves as a stress concentrator within the chitosan-lignin matrix. The  $p$ -value confirms that the observed difference is not due to random experimental variation but rather a systematic softening effect caused by microcapsule incorporation.<sup>49</sup> As reported in previous studies, microcapsule incorporation generally decreases in the fracture toughness values of the specimens. In this sense, other parameters, including microcapsule size, shell composition, aggregation effects, and structure-properties interaction related to oil-filled microcapsules, disrupt chain entanglement networks and create defect zones that amplify local stress fields. Similarly, the tensile strength in Fig. 7c decreased by 61.8%, from  $12.01 \pm 0.78 \text{ MPa}$  to  $4.59 \pm 0.12 \text{ MPa}$  ( $p = 8.1 \times 10^{-5}$ ). This reduction in tensile strength is attributed to the introduction of non-load-bearing microcapsular domains that disrupt the continuity of the polymer network, resulting in a lower load-bearing capacity. These significant  $p$ -values ( $< 0.001$ ) indicate a high level of confidence (greater than 99.9%) that the observed mechanical weakening arises directly from the incorporation of microcapsules. In contrast, ductility-related parameters showed significant improvement. The elongation at break presented in Fig. 7d more than doubled, increasing from  $16.03 \pm 1.70\%$  to  $34.97 \pm 2.85\%$  ( $p = 5.9 \times 10^{-4}$ ). This statistically significant increase ( $p < 0.001$ ) confirms that the microcapsules enhance film flexibility by facilitating plastic deformation of the polymer matrix. Similar behavior has been reported in previous studies,<sup>50,51</sup> where microcapsules exhibited elastic-plastic deformation under applied stress, allowing the material to undergo large plastic deformation without immediate fracture. Furthermore, interfacial interactions and chemical bonding between the capsule shells and the film matrix contribute to improved interfacial stability, enabling more effective stress distribution within the composite structure. The strain at yield in Fig. 7e increased moderately from  $3.02 \pm 0.11\%$  to  $3.71 \pm 0.30\%$  ( $p = 0.0202$ ), which remains statistically significant ( $p < 0.05$ ); this change indicates an improved ability of the material to absorb strain before permanent deformation. This result can be attributed to the disruption of polymer chain homogeneity caused by the presence of microcapsules, which facilitates chain slippage and mobility during stretching.<sup>52</sup> However, the toughness in Fig. 7f, calculated from the area under the stress-strain curve, decreased by approximately 22.3%, from  $127.82 \pm 5.83 \text{ mJ mm}^{-3}$  to  $99.27 \pm 4.70 \text{ mJ mm}^{-3}$  ( $p = 0.0027$ ). The statistical significance of this change ( $p < 0.01$ ) suggests that even though ductility increases, the overall capacity of the film to absorb energy before failure is statistically and mechanically reduced. This is consistent with SEM observations (Fig. 6), which revealed well-dispersed microcapsules and limited interfacial voids, suggesting partial compatibility and effective stress transfer at the capsule-matrix interface.<sup>53</sup> Collectively, these statistically validated results (all  $p \leq 0.05$ ) confirm that the observed mechanical differences are highly significant and reproducible across replicates. The consistent pattern of strong significance levels ( $p < 0.001$  for most parameters) underscores the reliability of the data and adherence to best statistical practices. The reduction in stiffness, accompanied by increased



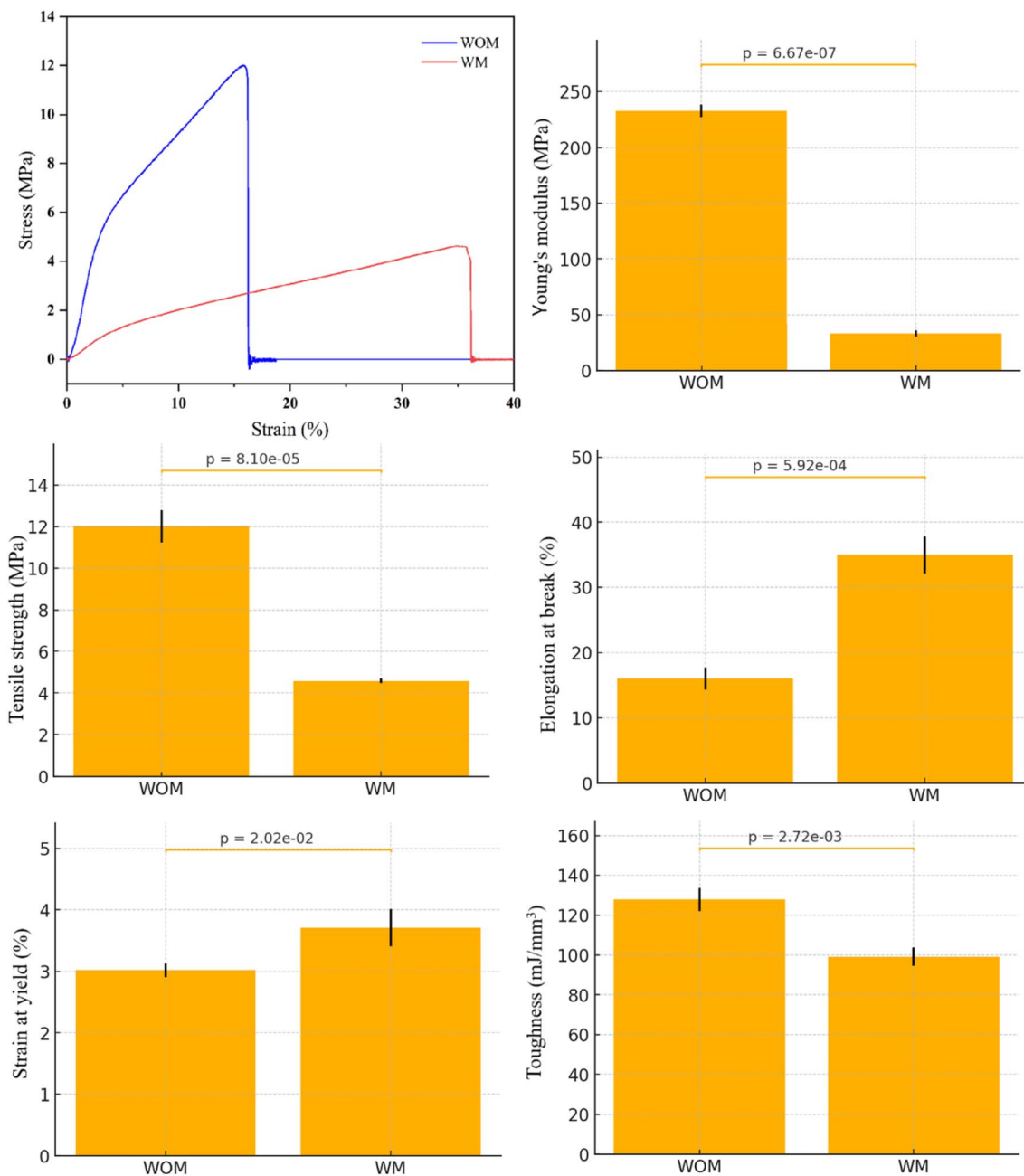


Fig. 7 Stress–strain curves obtained from tensile tests of the WOM and WM films.

elongation, supports the view that the microcapsules shell with gum Arabic behave as internal plasticizers, enhancing film flexibility, a desirable property for food packaging materials that must accommodate mechanical stress without fracturing.<sup>54,55</sup> Overall, the incorporation of alginate microcapsules successfully modulates the mechanical performance of the chitosan–lignin matrix, producing a more compliant and adaptable biopolymer film while maintaining sufficient mechanical integrity for packaging applications.

### Water swelling properties

The water-swelling properties of the WM and WOM films, as well as other biopolymer-based films, are governed by several

structural parameters, including the presence of hydrophilic functional groups ( $-\text{OH}$ ,  $-\text{NH}_2$ ), the degree of cross-linking between polymer chains, crystallinity, ionic strength, molecular weight, and molecular weight distribution. These factors collectively regulate the ability of the polymer matrix to absorb water and determine the balance between swelling behavior and water resistance.<sup>56</sup> Fig. 8 shows the maximum swelling capacity of the films when immersed in water at 7.23 pH. The WOM film exhibited a maximum swelling of 239.69 wt%, reflecting the high water-retention capacity of the chitosan–lignin matrix. This behavior can be attributed to the hydrophilic nature of chitosan and lignin, which contain abundant amino ( $-\text{NH}_2$ ) and hydroxyl ( $-\text{OH}$ ) functional groups capable of



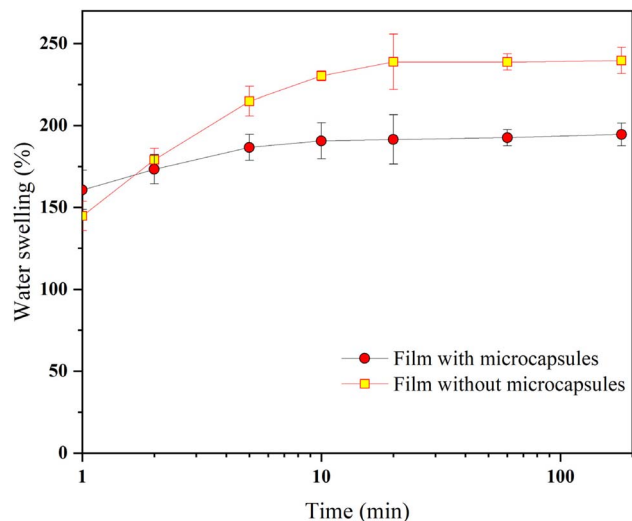


Fig. 8 Water swelling ratios of the films with and without microcapsules over 3 h.

forming strong hydrogen bonds with water molecules.<sup>57</sup> Chitosan, a natural polysaccharide widely used in biodegradable film development, is well known for its high swelling capacity, typically ranging between 200 and 600 wt%, due to the strong interaction between its functional groups and water molecules.<sup>58,59</sup> Moreover, the polar phenolic (–OH) and methoxy (–OCH<sub>3</sub>) groups present in lignin can further contribute to water affinity and swelling behavior. Similar swelling behavior has been reported in biopolymer systems containing water-soluble phytochemicals such as alkaloids, carbohydrates, tannins, and polyphenols.<sup>60</sup> However, the incorporation of microcapsules into the film matrix reduced the maximum swelling to 194.64 wt%. This decrease can be attributed to the presence of hydrophobic argan oil cores within the microcapsules, which partially occupy the polymer matrix and replace hydrophilic sites that would otherwise interact with water molecules. In addition, these hydrophobic domains create more tortuous diffusion pathways that hinder water penetration through the film structure. The alginate shells surrounding the oil cores may also contribute to this effect by forming additional barriers to water diffusion.<sup>61</sup> The observed reduction in swelling (approximately 19%) suggests improved water resistance of the composite film. Such behavior is advantageous for food packaging applications, where controlled moisture uptake and improved barrier properties are essential for maintaining film integrity, limiting microbial growth, and ultimately contributing to the extension of food shelf life.

### Antioxidant activity

The antioxidant effectiveness of the films, a key property for active food packaging, was quantitatively evaluated using the DPPH radical scavenging assay (Fig. 9). The results revealed a statistically significant increase in antioxidant activity after incorporation of argan oil microcapsules into the chitosan–lignin matrix. The chitosan film (CS) was used as the baseline to

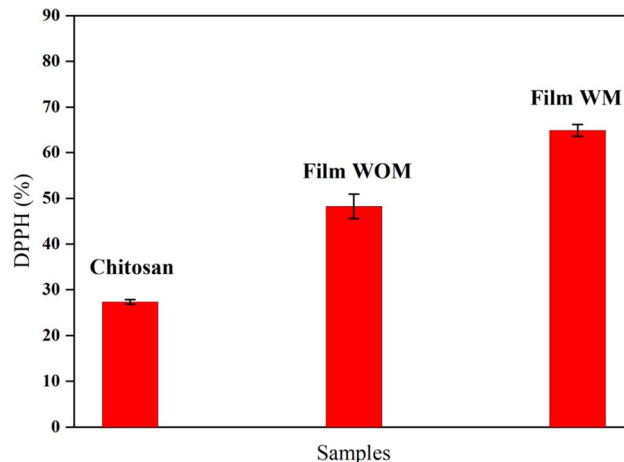


Fig. 9 Antioxidant activity of the films measured by the DPPH free radical scavenging assay.

evaluate the contribution of each component. The chitosan film exhibited a moderate DPPH scavenging activity of  $27.3 \pm 0.6\%$ . This intrinsic activity is attributed to the presence of free amino groups (–NH<sub>2</sub>) in the chitosan polymer, which can donate hydrogen atoms to stabilize and neutralize free radicals.<sup>62</sup> The incorporation of lignin (film WOM) resulted in a substantial increase in antioxidant capacity, reaching a scavenging activity of 48.3%. This improvement is associated with the high concentration of phenolic hydroxyl groups in lignin, which act as strong hydrogen donors and radical stabilizers capable of neutralizing free radicals and interrupting oxidative chain reactions.<sup>63</sup> Similar results were reported by Dghoughi, Raji, and Qaiss,<sup>64</sup> who demonstrated the superior antioxidant activity of lignin nanoparticles due to their high phenolic hydroxyl content, which enhances radical scavenging ability in DPPH and FRAP assays. The highest antioxidant activity was observed in the film containing argan oil microcapsules (film WM), which reached a scavenging activity of 64.6%, significantly higher than that of the chitosan–lignin film. This enhanced antioxidant performance can be attributed to the bioactive composition of argan oil, which contains high levels of phenolic compounds, flavonoids, and tannins.<sup>65</sup> Similar findings were reported by Kamal *et al.*,<sup>65</sup> who demonstrated that argan oil obtained by traditional hand-press extraction exhibits strong antioxidant activity due to its rich phenolic content. Comparable results were also reported by Cadi *et al.*,<sup>66</sup> who showed that argan oil derived from hand-pressed extraction has protective activity against H<sub>2</sub>O<sub>2</sub>-induced oxidative stress in *Tetrahymena pyriformis*. Furthermore, El Babili *et al.*<sup>67</sup> reported that *Argania spinosa* extracts exhibit promising antioxidant activity. In addition, our findings are consistent with the work of Amzal *et al.*,<sup>68</sup> who demonstrated that saponin compounds extracted from *A. spinosa* possess strong antioxidant properties. The highly significant *p*-values confirm that the incorporation of microcapsules not only preserves the antioxidant compounds present in argan oil but also facilitates their effective interaction with free radicals. Overall, the superior DPPH scavenging activity of the WM film highlights its strong potential as an



active packaging material capable of reducing oxidative degradation and extending the shelf life of oxidation-sensitive food products.<sup>69</sup>

### UV shielding

The combination of light and oxygen can accelerate the deterioration or spoilage of packaged food, mainly through lipid oxidation and the degradation of vitamins, pigments, and sensory quality. Ultraviolet (UV) radiation is particularly detrimental because its high energy can initiate photooxidative reactions, generating free radicals that accelerate fatty acid autoxidation and ultimately reduce food shelf life. Therefore, incorporating UV-blocking components into packaging materials is an effective strategy to protect food products from light-induced degradation and maintain their quality during storage.<sup>70</sup> UV filters in packaging materials absorb most of the incoming UV radiation, preventing it from reaching the food surface and thus limiting oxidative reactions.<sup>21,71</sup> In this study, the UV-visible absorption properties of the developed films were evaluated in three spectral regions: UVC (200–290 nm), UVB (290–320 nm), and UVA (320–400 nm). Fig. 10 presents the UV-vis spectra of alkali lignin, the film without microcapsules (WOM), and the film containing microcapsules (WM). As presented in the figure, alkali lignin exhibits exceptional UV-shielding properties due to its rich content of aromatic rings, phenolic hydroxyl groups, and conjugated chromophoric structures that strongly absorb ultraviolet radiation across UVC (200–290 nm), UVB (290–320 nm), and UVA (320–400 nm) regions.<sup>72</sup> On the same figure, the WOM film exhibited the highest absorbance across the UV region, with characteristic peaks near 280 nm, corresponding to  $\pi \rightarrow \pi^*$  transitions of aromatic rings, and around 320 nm, associated with phenolic structures. These chromophoric groups enable nearly complete UV blocking (>99%) up to ~580 nm, with absorbance values typically reaching 3.5–4.0 A.U., indicating almost complete protection against UV radiation. Beyond this wavelength,

absorbance decreased sharply, reaching about 1.65 A.U. at 800 nm, reflecting increased light transmission in the visible region. This strong UV-blocking performance is primarily attributed to the opacity effect of lignin, which is primarily responsible for UV absorption in the film.<sup>73</sup> Chitosan contributes negligible UV absorption (<1.0 A.U.), consistent with literature reports showing that pure chitosan films exhibit low UV-B and UVA blocking efficiencies, confirming that lignin is the primary UV-shielding component (>95% absorbance across UVC, UVB, and UVA).<sup>74</sup> Lignin contains aromatic rings, phenolic hydroxyl groups, and conjugated chromophoric structures, which strongly absorb UV radiation and dissipate the absorbed energy through non-radiative processes.<sup>75</sup> When argan oil microcapsules were incorporated into the film (WM), the main UV absorption region shifted slightly from 200–580 nm (WOM) to approximately 200–570 nm, while the maximum absorbance remained high at 3.9–4.0 A.U. across the UV ranges, representing a minor reduction ( $\leq 6\%$ , non-significant,  $p > 0.05$ ). This subtle change likely arises from light-scattering effects introduced by the microcapsules within the film matrix.<sup>76</sup> Specifically, scattering occurs at the interfaces between the microcapsules and the matrix, where incident light is partially redirected rather than transmitted directly through the film.<sup>77</sup> This phenomenon reduces overall transparency and slightly compresses the absorption edge by approximately 10 nm. After 570 nm, the WM film also showed a sharp decrease in absorbance, approaching about 1.7 A.U. at 800 nm, indicating that both films retain partial transparency in the visible region while still providing strong UV protection.<sup>78</sup> Overall, the remarkable UV-blocking ability of these films can be mainly attributed to the presence of lignin within the film matrix, which acts as the primary UV absorber. The contribution of bioactive compounds from encapsulated argan oil may further enhance the functional performance of the film. Consequently, the developed films demonstrate strong potential for active food-packaging applications, where protection against UV-induced oxidation is essential for preserving food quality and extending shelf life.

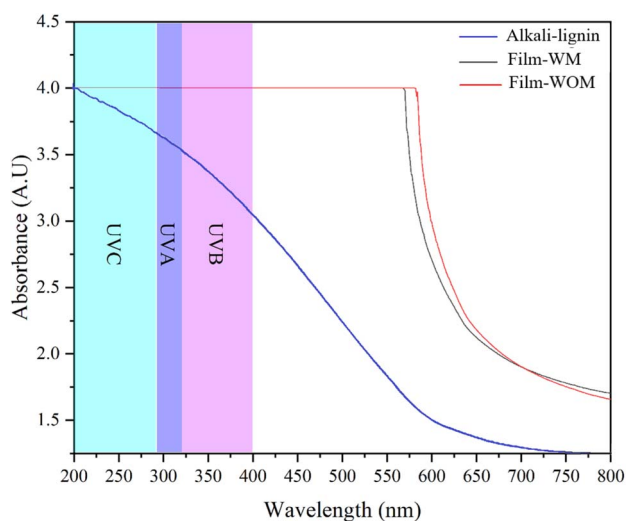


Fig. 10 UV absorption of alkali lignin and films with and without microcapsules.

### Antibacterial properties

Fig. 11 presents the antibacterial activity of lignin–chitosan films (Lig-C, reference) and lignin–chitosan films containing argan oil microcapsules (Lig-CM) against *Staphylococcus aureus*, *Pseudomonas aeruginosa*, and *Escherichia coli*. The evaluation followed a modified version of ISO 22196:2011,<sup>79</sup> quantifying bacterial survival (CFU mL<sup>-1</sup> cm<sup>-2</sup>) on the film surface after incubation rather than measuring inhibition zones. This contact-based method is particularly suitable for polymeric films containing embedded antimicrobial agents, where activity occurs mainly at the film–bacteria interface rather than through diffusion into agar. In the first assay using 6 mm diameter film discs, Lig-CM films showed a moderate reduction in bacterial counts compared with Lig-C films, especially for *E. coli* (from  $21 \times 10^7$  to  $8.6 \times 10^7$  CFU mL<sup>-1</sup> cm<sup>-2</sup>) and *S. aureus* (from  $16.6 \times 10^7$  to  $9.0 \times 10^7$  CFU mL<sup>-1</sup> cm<sup>-2</sup>). This reduction suggests a partial antibacterial effect attributable to the combination of chitosan and bioactive compounds in argan oil



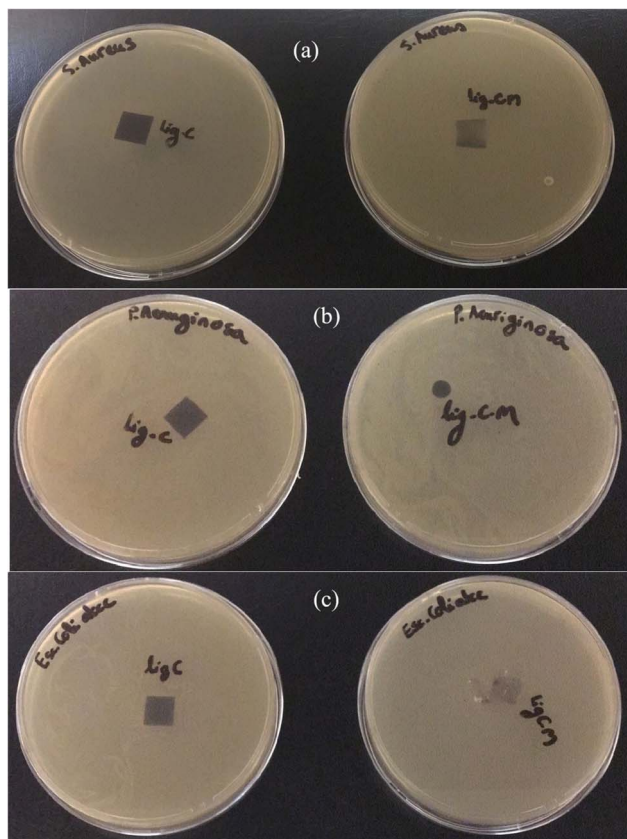


Fig. 11 Antibacterial activities of the film with microcapsules on the right and the film without microcapsules on the left against (a) *Staphylococcus aureus*, (b) *Pseudomonas aeruginosa*, and (c) *Escherichia coli*.

microcapsules.<sup>80,81</sup> Chitosan contributes electrostatic interactions *via* its protonated amino groups, destabilizing bacterial membranes, while hydrophobic phenolic and lipid constituents of argan oil enhance membrane penetration, like the dual-action mechanism of long-chain quaternary ammonium compounds.<sup>82</sup> For *Pseudomonas aeruginosa*, both Lig-C and Lig-CM films demonstrated contact-active antimicrobial activity, as reflected by bacterial reductions at the film surface. Although no inhibition halos were observed in agar, this is consistent with previous reports where contact-active antimicrobial polymers exhibit localized bacterial killing without diffusion into surrounding media. This indicates a synergistic effect of the cationic chitosan matrix and encapsulated argan oil compounds on bacterial membranes upon direct contact, even for Gram-negative strains with outer membrane protection. In the second assay using larger 1 cm<sup>2</sup> film samples, both Lig-C and Lig-CM films showed high bacterial loads for *E. coli* and *S. aureus*, further supporting that the antimicrobial activity is primarily contact-dependent rather than diffusion-mediated. The absence of visible inhibition zones is therefore expected and does not reflect a lack of activity. Overall, the moderate antibacterial effect of Lig-CM films can be attributed to the relatively low argan oil loading (~4.5 wt%) and controlled release from microcapsules, which limits rapid antimicrobial

availability.<sup>83</sup> Nevertheless, the partial reduction observed, particularly against *S. aureus*, and the contact-active effects against *P. aeruginosa*, suggest that Lig-CM films may offer functional benefits in real food packaging.<sup>54</sup> Depending on the methodology used, such as disk diffusion or broth quantitative assays, biodegradable films containing bioactive agents, including silver nanoparticles (AgNPs) or essential oils, can display antibacterial activity that is often contact-dependent. In our study, Lig-CM films containing argan oil microcapsules showed moderate antibacterial effects primarily at the film-bacteria interface, while visual inhibition halos in agar plates were absent or minimal, consistent with a contact-active mechanism. Similarly, in studies on AgNP-based films,<sup>84,85</sup> the agar diffusion assay showed bacterial inhibition in areas directly contacting the film, and only small or absent clear zones were observed around the film. Abreu *et al.*<sup>86</sup> reported that bacterial inhibition occurred in contact areas with AgNP films, despite no inhibition halo being visible. Comparable observations have been made with silver nanoparticles in liquid suspensions plated directly onto bacterial lawns,<sup>87,88</sup> demonstrating that the polymer matrix or medium often limits diffusion and therefore halo formation. These findings highlight that the absence of an inhibition halo does not indicate a lack of antimicrobial activity but rather reflects the restricted migration of hydrophobic or particulate antimicrobial agents in agar.<sup>89</sup> Packaging application provides a more reliable assessment of antibacterial performance for polymer films, allowing for mechanistic insights and practical evaluation of their potential in real-world applications, including food packaging.

### Packaging ability

The biological composition of fresh meat products makes them highly susceptible to spoilage. Fresh meat typically contains 12–20% protein, 0–6% carbohydrates, and 3–45% fat.<sup>90</sup> One of the main mechanisms responsible for meat deterioration is the oxidation of fatty acids, which occurs when lipids react with oxygen, leading to degradation of the fats present in meat.<sup>91</sup> Fatty acids in meat are primarily present as triglycerides, composed of glycerol molecules esterified with three fatty acid chains.<sup>92</sup> When meat is exposed to oxygen, the oxygen molecules interact with unsaturated fatty acids in triglycerides, initiating a chain reaction known as lipid oxidation. During this process, oxygen reacts with unsaturated fatty acids to generate free radicals, which are highly reactive species capable of propagating further oxidative reactions.<sup>91,93</sup> Lipid oxidation not only causes quality deterioration but can also promote bacterial growth by providing energy and carbon sources for microorganisms.<sup>94,95</sup> However, the incorporation of natural antioxidants, such as those present in argan oil, or synthetic antioxidants into meat products can inhibit oxidation by scavenging free radicals, thereby preventing the formation of oxidation products and reducing microbial proliferation.<sup>96</sup>

Fig. 12 illustrates the effect of incorporating microcapsules into the packaging film on bacterial growth in ground meat during a storage period of three days. The images on the left correspond to films without microcapsules (WOM), whereas



Table 2 Color change of ground meat packaged with the film without microcapsules and the film with microcapsules for 3 days









Composite films	0 day	1 day	2 days	3 days
WOM				
CIE $L^*a^*b^*$	52, 19, 16	26, 11, -2	28, 7, 2	33, 7, 6
WM				
CIE $L^*a^*b^*$	50, 25, 20	15, 16, 5	14, 15, 7	21, 5, 3

Table 3 Comparison of the performance of intelligent packaging with different systems

Film type	DPPH scavenging activity	Antibacterial activity ( <i>S. aureus</i> )	Tensile strength (MPa)	Young's modulus (MPa)	Reference
WM film + argan oil (this study)	64.6%	Reduced CFU from $16.6 \times 10^7$ to $9.0 \times 10^7$ (ISO 22196)	4.59	33.14	This study
Chitosan + thyme EO nanoemulsion	Improved vs. control	Clear inhibition zone (8 mm well method)	$10.79 \pm 2.82$	Not reported	55
Chitosan + gallic acid (1.5 mM)	13.5 mg TE $g^{-1}$ film	Reported effective	Not reported	Not reported	98
Chitosan + flavonols	80%	90%	Not reported	Not reported	99
Chitosan + tea tree EO (TTEO)	$61.24 \pm 0.64\%$	Not reported	1.54–4.23	1.81–2.96	97
Chitosan + clove EO-HP- $\beta$ -CD complex	88%	Not reported	Moderate (burst strength: $\sim 8.41$ N)	Not reported	53

those on the right correspond to films containing microcapsules (WM). The upper row shows the samples on Day 0, while the lower row shows the samples after three days of storage. The extent of surface bacterial growth and meat discoloration was used as a qualitative indicator of the antibacterial performance of the films, and the percentage of the meat surface covered by bacterial growth was quantified over three days using ImageJ image analysis software. On Day 1, no visible bacterial growth was detected on the surface of either sample. However, the WOM sample exhibited the appearance of a shiny surface, which may indicate early signs of spoilage. By Day 2, the WM film limited bacterial spread to 12.3% surface coverage, whereas the WOM film showed 26.7% coverage. Herein, the influence of microcapsules became more pronounced. The meat packaged with the WM film still exhibited limited bacterial development, whereas the sample packaged with the WOM film showed a thicker bacterial layer and more evident surface deterioration. On Day 3, the bacterial coverage increased to 26.3% for the WM sample, while the WOM sample reached 33.4%, indicating more extensive microbial growth. These results suggest that the incorporation of microcapsules delayed bacterial growth in the meat by approximately one day. This behavior can be attributed

to the antioxidant compounds present in the argan oil core of the microcapsules, which help slow oxidative degradation and limit bacterial proliferation, demonstrating the potential antimicrobial effect of the active film. However, it should be noted that quantitative microbiological analyses and chemical spoilage indicators would be required to definitively confirm shelf-life extension under commercial refrigerated storage conditions. The WM film developed in this study, based on a chitosan–lignin matrix incorporating microencapsulated argan oil, exhibits a well-balanced performance in terms of antioxidant, antimicrobial, and mechanical properties. With a DPPH radical scavenging activity of 64.6%, the film demonstrates strong antioxidant potential, surpassing several comparable systems such as chitosan films containing tea tree essential oil (61.2%)<sup>97</sup> and gallic acid-based systems (13.5 mg TE  $g^{-1}$  film).<sup>98</sup> Although slightly lower than the maximum values reported for films incorporating clove essential oil-cyclodextrin complexes (88%)<sup>53</sup> or flavonols (80%),<sup>99</sup> the present formulation achieves this performance using a relatively low concentration of active oil ( $\sim 4.5$  wt%, see Table 2). This indicates an efficient antioxidant delivery system enabled by microencapsulation and the synergistic contribution of lignin's polyphenolic structure.



Table 2 highlights the effect of the composite films on the color stability of ground meat during storage for three days. Meat packaged with WM films (lignin–chitosan films containing argan oil microcapsules) showed a slower deterioration of color compared with the WOM control films. For the WOM samples, the redness parameter ( $a^*$ ) decreased markedly from 19 to 7 over the storage period (around 63% reduction), while the lightness ( $L^*$ ) dropped sharply during the first day (52 to 26), indicating rapid surface darkening. At the same time, the increase in the  $b^*$  coordinate ( $-2$  to  $6$ ) suggests progressive yellow–brown discoloration, which is typical of the oxidation of Myoglobin into Metmyoglobin. These changes indicate significant color deterioration and loss of the characteristic bright red

appearance expected for fresh meat. In contrast, samples packaged with WM films exhibited a comparatively slower decline in color quality. Although a reduction in redness was also observed ( $a^*$ : 25 to 5), the presence of lignin–chitosan and encapsulated argan oil appeared to delay discoloration during the early storage stages, as evidenced by the higher initial redness values and a more gradual shift in the CIE  $L^*a^*b^*$  parameters. The evolution of the  $b^*$  values (20 to 3) further suggests that the WM film limited the development of yellow–brown tones associated with oxidative degradation. This improved stability can be attributed to the antioxidant activity of argan oil constituents, particularly tocopherols and phenolic compounds, which inhibit lipid oxidation and reduce the formation of secondary oxidation products, such as malondialdehyde, which accelerate pigment oxidation. Similar results in the works by Dera *et al.*<sup>100</sup> and Kanatt *et al.*<sup>100</sup> reported antioxidant properties of chitosan films on meat. In the present study, even the control group, which contained chitosan without EO, presented decreased  $L^*$  values (approximately 5 units) and maintained  $a^*$  values, due to the oxidation of Hemopigments, leading to gradual discoloration of the meat. The antioxidant properties of chitosan were improved by EO addition, as color parameters were better preserved in the presence of EOs. Overall, the results indicate that incorporating argan oil microcapsules within the lignin–chitosan matrix contributes to a protective effect against oxidative discoloration of meat. By slowing the conversion of oxymyoglobin to metmyoglobin, the WM films help maintain the desirable red appearance of ground meat for a longer period compared with the control films, suggesting their potential as active packaging materials for extending the visual quality of fresh meat products. Table 3 presents a comparison of the performance of intelligent packaging with different systems. The antimicrobial performance of the WM film was also evaluated using the ISO 22196 standardized methodology, which revealed a 45.7% reduction in *S. aureus* (from  $16.6 \times 10^7$  to  $9.0 \times 10^7$  CFU mL<sup>-1</sup> cm<sup>-2</sup>). The use of microcapsules enables the controlled release of bioactive compounds, potentially contributing to sustained antimicrobial activity during storage. From a mechanical standpoint, although the tensile strength of the WM film (4.59 MPa) is slightly lower than that reported for some films without encapsulated oil (*e.g.*, chitosan–thyme essential oil nano-emulsion films at 10.79 MPa),<sup>55</sup> it remains within a suitable range for flexible packaging applications. Furthermore, the film exhibits a Young's modulus of 33.14 MPa, indicating moderate flexibility and structural resilience, which is advantageous compared with several essential oil-based systems where excessive plasticization can compromise film stiffness and handling. Overall, the WM film represents a functionally promising and environmentally sustainable packaging material, combining bio-based components, controlled release of active compounds, and balanced physicochemical properties. These characteristics highlight its potential as an active food packaging system for improving the preservation of perishable products.

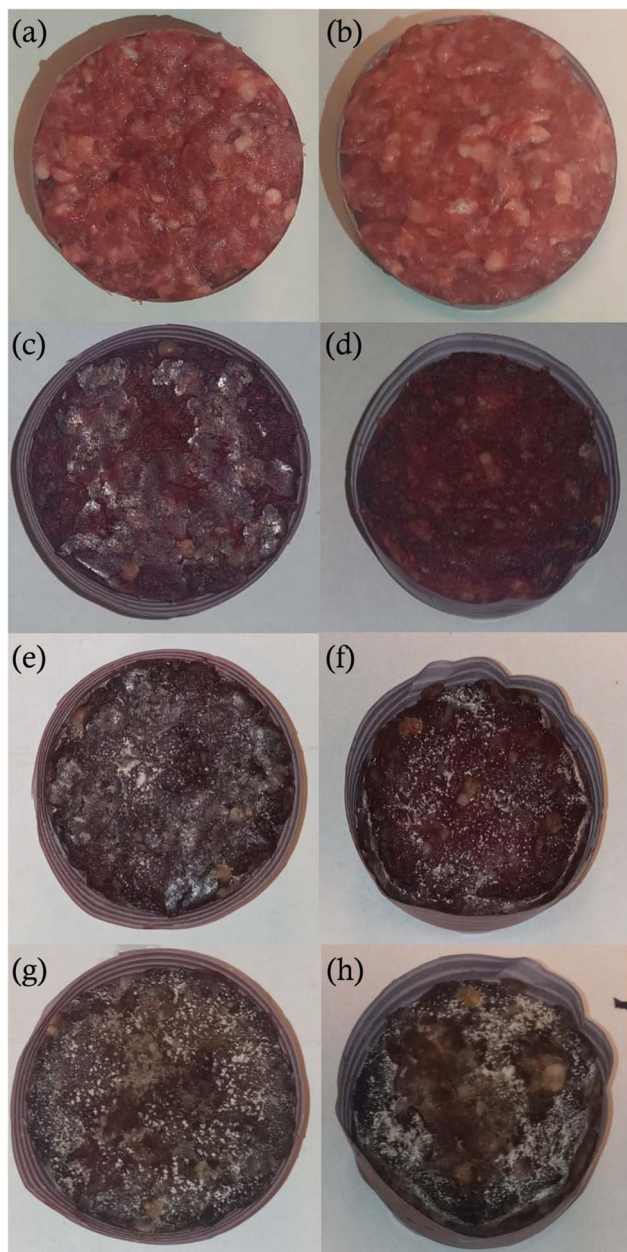


Fig. 12 Ground meat packaged with (a, c, e and g) the film without microcapsules and (b, d, f and h) the film with microcapsules for 3 days.



## Conclusion

This study reports the successful development of an active, bio-based packaging film based on a chitosan–lignin matrix incorporating alginate microcapsules loaded with argan oil, using gum arabic as an emulsifying agent. Structural and morphological analyses (FTIR, SEM, TGA) confirmed efficient encapsulation and good compatibility of the microcapsules within the polymeric matrix. Incorporation of argan oil microcapsules enhanced the functional properties of the films. Antioxidant activity increased from 48.3% to 64.6% (DPPH assay), reflecting the contribution of bioactive compounds such as tocopherols and phenolics. Moderate antibacterial activity against *Staphylococcus aureus* and *Escherichia coli* was observed, indicating synergistic effects between chitosan, lignin, and encapsulated oil. Mechanically, microcapsules reduced tensile strength and stiffness but improved flexibility, as evidenced by higher elongation at break. Both films exhibited strong UV-blocking capacity due to lignin's aromatic structure, offering protection against photo-induced degradation. Application tests on ground meat under refrigerated storage showed that the active film better preserved color and visual quality, extending shelf life by approximately one day. These results demonstrate the potential of chitosan–lignin films with argan oil microcapsules as sustainable, functional, active packaging materials. However, the study has limitations. Antimicrobial activity was not quantified by microbial enumeration, and lipid oxidation was not measured using standard markers (e.g., TBARS). Storage trials were limited in duration and conducted under controlled conditions. Future studies should focus on quantitative microbiological and oxidation analyses, extended storage tests, release kinetics of encapsulated compounds, and validation under real industrial conditions.

## Consent to participate

This research does not address human subjects, so we do not need informed consent to participate.

## Consent to publish

All the authors have reviewed and approved the manuscript being submitted. We warrant that the article is the author's original work. We affirm that the article has not received prior publication and is not under consideration for publication elsewhere. On behalf of all coauthors, the corresponding author bears full responsibility for the submission.

## Author contributions

Abdellah Halloub wrote the manuscript, conceived, planned the experiments, and discussed the results. Marya Raji wrote the manuscript, conceived and planned the experiments, conceived the original idea, discussed the results, and contributed to the final manuscript.

## Conflicts of interest

There are no conflicts to declare.

## Data availability

The data supporting the findings of this study are available within the article. Additional data, including raw and processed datasets, characterization results (FTIR, SEM, TGA, etc.), and analytical measurements, are available from the corresponding author upon reasonable request.

## Acknowledgements

This work was funded by the Moroccan Ministry of Higher Education, Scientific Research, and Innovation (MHESRI-M) under Convention 2023 (MESRI-UM-P) No. 12 through the QUIPACK-PRIMA project and supported by Mohammed VI Polytechnic University (UM6P). The authors also acknowledge the MAScIR Foundation for providing part of the research environment in which this work was conducted. The authors further thank Dr Nawal Merghoub for her assistance with the antibacterial activity tests.

## References

- 1 J. Gustavsson, *Global Food Losses and Food Waste : Extent, Causes and Prevention: Study Conducted for the International Congress 'Save Food!' at Interpack 2011 Düsseldorf, Germany*, Food and Agriculture Organization of the United Nations, 2011.
- 2 H. Mehlhorn, *WHO Estimates of the Global Burden of Foodborne Diseases: Foodborne Disease Burden Epidemiology Reference Group 2007-2015*, World Health Organization, Geneva, 2015.
- 3 M. Raji, A. Halloub, A. el Kacem Qaiss and R. Bouhfid, in *Handbook of Bioplastics and Biocomposites Engineering Applications*, ed. T. A. Inamuddin, Wiley, 2nd edn., 2023, pp. 457–470.
- 4 T. B. Jeffrey, *FSMA and Food Safety Systems Understanding and Implementing the Rules*, Barach Enterprises, LLC, Chichester, 2016.
- 5 M. Raji, L. El Foujji, M. E. M. Mekhzoum, M. El Achaby, H. Essabir, R. Bouhfid and A. el kacem Qaiss, pH-indicative Films Based on Chitosan–PVA/Sepiolite and Anthocyanin from Red Cabbage: Application in Milk Packaging, *J. Bionic Eng.*, 2022, **19**, 837–851.
- 6 R. Domínguez, F. J. Barba, B. Gómez, P. Putnik, D. Bursac Kovačević, M. Pateiro, E. M. Santos and J. M. Lorenzo, Active packaging films with natural antioxidants to be used in meat industry: a review, *Food Res. Int.*, 2018, **113**, 93–101.
- 7 M. Vinceković, M. Viskić, S. Jurić, J. Giacometti, D. Bursac Kovačević, P. Putnik, F. Donsi, F. J. Barba and A. Režek Jambrak, Innovative technologies for encapsulation of Mediterranean plants extracts, *Trends Food Sci. Technol.*, 2017, **69**, 1–12.



- 8 Z. C. Wang, Y. Lu, Y. Yan, T. Nisar, Z. Fang, N. Xia, Y. Guo and D. W. Chen, Effective inhibition and simplified detection of lipid oxidation in tilapia (*Oreochromis niloticus*) fillets during ice storage, *Aquaculture*, 2019, DOI: [10.1016/j.aquaculture.2019.05.068](https://doi.org/10.1016/j.aquaculture.2019.05.068).
- 9 F.-L. Juana and M. Viuda-martos, Introduction to the Special Issue: Application of Essential Oils in Food Systems, *Foods*, 2018, DOI: [10.3390/foods7040056](https://doi.org/10.3390/foods7040056).
- 10 M. Raji, H. Essabir, M. ElAchaby, R. Bouhfid and A. Qaiss, Morphology control of poly(lactic) acid/polypropylene blend composite by using silanized cellulose fibers extracted from coir fibers, *Cellulose*, 2022, **29**, 6759–6782.
- 11 A. El Abbassi, N. Khalid, H. Zbakh, A. Ahmad, A. E. L. Abbassi, N. Khalid and H. Zbakh, Physicochemical characteristics, nutritional properties, and health benefits of argan oil: a review, *Crit. Rev. Food Sci. Nutr.*, 2014, **54**, 1401–1414.
- 12 A. Dghoughi, M. Raji, H. Chakchak, M. O. Bensalah, R. Bouhfid and A. E. K. Qaiss, Synthesis of triangular lignin photonic crystal nanoparticles: investigating solvent effects and dialysis optimization, *Int. J. Biol. Macromol.*, 2025, **291**, 139110.
- 13 M. Bakour, N. Soulo, N. Hammas, H. El Fatemi, A. Aboulghazi, A. Taroq, A. Abdellaoui, N. Al-Waili and B. Lyoussi, The antioxidant content and protective effect of argan oil and syzygium aromaticum essential oil in hydrogen peroxide-induced biochemical and histological changes, *Int. J. Mol. Sci.*, 2018, DOI: [10.3390/ijms19020610](https://doi.org/10.3390/ijms19020610).
- 14 C. Cabrera-Vique, R. Marfil, R. Giménez and O. Martínez-Augustin, Bioactive compounds and nutritional significance of virgin argan oil – an edible oil with potential as a functional food, *Nutr. Rev.*, 2012, **70**, 266–279.
- 15 N. M. H. Khong and K. W. Chan, Biological activities of argan (*Argania spinosa* L.) oil: Evidences from in vivo studies; in Multiple Biological Activities of Unconventional Seed, *Oils*, 2022.
- 16 S. Gharby and Z. Charrouf, Argan Oil Chemical Composition, Extraction Process, and Quality Control, *Front. Nutr.*, 2022, **8**, 804587.
- 17 R. El Kebbaj, H. Bouchab, M. Tahri-Joutey, S. Rabbaa, Y. Limami, B. Nasser, M. C. Egbujor, P. Tucci, P. Andreoletti, L. Saso and M. Cherkaoui-Malki, The Potential Role of Major Argan Oil Compounds as Nrf2 Regulators and Their Antioxidant Effects, *Antioxidants*, 2024, 344.
- 18 C. D. Petcu, D. Tăpăloagă, O. D. Mihai, R. A. Gheorgher-Imiria, C. Negoită and I. M. Petcu, Harnessing Natural Antioxidants for Enhancing Food Shelf Life: Exploring Sources and Applications in the Food Industry, *Foods*, 2023, **12**, 3176.
- 19 H. El Monfalouti, D. Guillaume, C. Denhez and Z. Charrouf, Therapeutic potential of argan oil: a review, *J. Pharm. Pharmacol.*, 2010, **62**(12), 1669–1675.
- 20 Z. Charrouf and D. Guillaume, Argan oil: Occurrence, composition and impact on human health, *Eur. J. Lipid Sci. Technol.*, 2008, **110**, 632–636.
- 21 A. Halloub, M. Raji, H. Essabir, H. Chakchak, M. Bensalah and R. Bouhfid, Intelligent food packaging film containing lignin and cellulose nanocrystals for shelf life extension of food, *Carbohydr. Polym.*, 2022, **296**, 119972.
- 22 A. Halloub, S. Nekhlaoui, M. Raji, H. Essabir, M. ouadi Bensalah, R. Bouhfid and A. E. kacem Qaiss, UV-activated self-healing food packaging:  $\omega$ -3 based microcapsules in hemicellulose/chitosan blend film for cashew nut preservation, *Food Biosci.*, 2024, **60**, 104313.
- 23 M. C. S. Aguiar, M. F. das Graças Fernandes da Silva, J. B. Fernandes and M. R. Forim, Evaluation of the microencapsulation of orange essential oil in biopolymers by using a spray-drying process, *Sci. Rep.*, 2020, **10**, 11799.
- 24 K. Sharad, H. Izharul, Y. Ashutosh, P. Jyoti and A. Raj, Immobilization and Biochemical Properties of Purified Xylanase from *Bacillus amyloliquefaciens* SK-3 and Its Application in Kraft Pulp Biobleaching, *J. Clin. Microbiol. Biochem. Technol.*, 2016, **2**, 026–034.
- 25 Y. Q. Almulaiky and S. A. Al-Harbi, Preparation of a calcium alginate-coated polypyrrole/silver nanocomposite for site-specific immobilization of polygalacturonase with high reusability and enhanced stability, *Catal. Lett.*, 2022, **152**, 28–42.
- 26 H. Yang, J. Irudayaraj and M. M. Paradkar, Discriminant analysis of edible oils and fats by FTIR, FT-NIR and FT-Raman spectroscopy, *Food Chem.*, 2005, **93**, 25–32.
- 27 M. Kharbach, R. Kamal, M. Bousrabat, M. Alaoui Mansouri, I. Barra, K. Alaoui, Y. Cherrah, Y. Vander Heyden and A. Bouklouze, Characterization and classification of PGI Moroccan Argan oils based on their FTIR fingerprints and chemical composition, *Chemom. Intell. Lab. Syst.*, 2017, **162**, 182–190.
- 28 A. Hassani, S. Mahmood, H. H. Enezei, S. A. Hussain, H. A. Hamad, A. F. Aldoghachi, A. Hagar, A. A. Doolaanea and W. N. Ibrahim, Formulation, characterization and biological activity screening of sodium alginate-gum Arabic nanoparticles loaded with curcumin, *Molecules*, 2020, **25**, 2244, DOI: [10.3390/molecules25092244](https://doi.org/10.3390/molecules25092244).
- 29 K. Madhusudana Rao, K. S. V. Krishna Rao, P. Sudhakar, K. Chowdoji Rao and M. C. S. Subha, Synthesis and characterization of biodegradable poly (vinyl caprolactam) grafted on to sodium alginate and its microgels for controlled release studies of an anticancer drug, *J. Appl. Pharm. Sci.*, 2013, **3**, 61–69.
- 30 R. A. Nandanwar, A. R. Chaudhari and J. D. Ekhe, Nitrobenzene oxidation for isolation of value added products from industrial waste lignin, *J. Chem. Bio. Phy. Sci. Sec. D*, 2016, **6**, 501–513.
- 31 V. Nair, A. Panigrahy and R. Vinu, Development of novel chitosan-lignin composites for adsorption of dyes and metal ions from wastewater, *Chem. Eng. J.*, 2014, **254**, 491–502.
- 32 S. Sohni, R. Hashim, H. Nidaullah, J. Lamaming and O. Sulaiman, Chitosan/nano-lignin based composite as a new sorbent for enhanced removal of dye pollution from aqueous solutions, *Int. J. Biol. Macromol.*, 2019, **132**, 1304–1317.



- 33 S. Elshamy, K. Khadizatul, K. Uemura, M. Nakajima and M. A. Neves, Chitosan-based film incorporated with essential oil nanoemulsion foreseeing enhanced antimicrobial effect, *J. Food Sci. Technol.*, 2021, **58**, 3314–3327.
- 34 A. Zerouh, L. Belkbir and B. Fdili Alaoui, Conservation Study of the Argan Oil by Thermogravimetry, *Asian J. Chem.*, 2001, **13**, 144–150.
- 35 A. P. Esser-Kahn, S. A. Odom, N. R. Sottos, S. R. White and J. S. Moore, Triggered Release from Polymer Capsules, *Macromolecules*, 2011, **44**, 5539–5553.
- 36 K. B. Fujiu, I. Kobayashi, M. A. Neves, K. Uemura and M. Nakajima, Influence of temperature on production of water-in-oil emulsions by microchannel emulsification, *Colloids Surf., A*, 2012, **411**, 50–59.
- 37 S. Zhao, R. Wang, Y. Xu, C. Wang, J. Xu, P. Wang, Y. Fu, J. Su, H. Chai, J. He and H. Chen, The Effect of Polysaccharide Colloids on the Thermal Stability of Water-in-Oil Emulsions, *Polymers*, 2025, **17**, DOI: [10.3390/polym17060809](https://doi.org/10.3390/polym17060809).
- 38 C. Guzmán-Pincheira, A. Moeini, P. E. Oliveira, D. Abril, Y. A. Paredes-Padilla and S. Benavides-Valenzuela, Development of Alginate-Chitosan Bioactive Films Containing Essential Oils for Use in Food Packaging, *Foods*, 2025, **14**, 1.
- 39 B. Deepa, E. Abraham, L. A. Pothan, N. Cordeiro, M. Faria and S. Thomas, Biodegradable Nanocomposite Films Based on Sodium Alginate and Cellulose Nanofibrils, *Materials*, 2016, **9**, 1–11.
- 40 A. Salisu, M. M. Sanagi, A. Abu Naim, K. J. Abd Karim, W. A. Wan Ibrahim and U. Abdulganiyu, Alginate graft polyacrylonitrile beads for the removal of lead from aqueous solutions, *Polym. Bull.*, 2016, **73**, 519–537.
- 41 Z. Ma, Q. Sun, J. Ye, Q. Yao and C. Zhao, Study on the thermal degradation behaviors and kinetics of alkali lignin for production of phenolic-rich bio-oil using TGA-FTIR and Py-GC/MS, *J. Anal. Appl. Pyrolysis*, 2016, **117**, 116–124.
- 42 K. Ravishankar, M. Venkatesan, R. P. Desingh, A. Mahalingam, B. Sadhasivam, R. Subramaniyam and R. Dhamodharan, Biocompatible hydrogels of chitosan-alkali lignin for potential wound healing applications, *Mater. Sci. Eng., C*, 2019, **102**, 447–457.
- 43 I. L. Hia, P. Pasbakhsh, E. S. Chan and S. P. Chai, Electrospayed Multi-Core Alginate Microcapsules as Novel Self-Healing Containers OPEN, *Sci. Rep.*, 2016, **6**, 1–8.
- 44 E. A. Soliman, A. Y. El-Moghazy, M. S. M. El-Din, M. A. Massoud, E. A. Soliman, A. Y. El-Moghazy, M. S. M. El-Din and M. A. Massoud, Microencapsulation of Essential Oils within Alginate: Formulation and in Vitro Evaluation of Antifungal Activity, *J. Encapsulation Adsorpt. Sci.*, 2013, **3**, 48–55.
- 45 W. Jiang, X. Guan, L. Wang, Y. Mao, P. Ma, W. Liu, Y. Li, T. Ngai and H. Jiang, Fabrication of Porous Proteinaceous Microspheres via One-Step Pickering Double Emulsions: Controllable Structure and Interfacial Cascade Biocatalysis, *Langmuir*, 2025, **41**, 7302–7311.
- 46 J. D. Lavertu, K. K. Bawa, S. Hrapovic, D. Fu, J. K. Oh and U. D. Hemraz, Fabrication of thermo-responsive multicore microcapsules using a facile extrusion process, *RSC Adv.*, 2024, **14**, 20105–20112.
- 47 L. Huang, K. Wu, R. Zhang and H. Ji, Fabrication of Multicore Milli- and Microcapsules for Controlling Hydrophobic Drugs Release Using a Facile Approach, *Ind. Eng. Chem. Res.*, 2019, **58**, 17017–17026.
- 48 I. L. Hia, W. H. Lam, S. P. Chai, E. S. Chan and P. Pasbakhsh, Surface modified alginate multicore microcapsules and their application in self-healing epoxy coatings for metallic protection, *Mater. Chem. Phys.*, 2018, **215**, 69–80.
- 49 S. Vigneshwaran, M. Uthayakumar and V. Arumugaprabu, A review on erosion studies of fiber-reinforced polymer composites, *J. Reinf. Plast. Compos.*, 2017, **36**, 1019–1027.
- 50 J. F. Su, J. Qiu and E. Schlangen, Stability investigation of self-healing microcapsules containing rejuvenator for bitumen, *Polym. Degrad. Stab.*, 2013, **98**, 1205–1215.
- 51 T. Wang, Z. Yang, C. Zhang, X. Zhai, X. Zhang, X. Huang, Z. Li, X. Zhang, X. Zou and J. Shi, Chitosan-cinnamom essential oil/sodium alginate-TiO<sub>2</sub> bilayer films with enhanced bioactive retention property: application for mango preservation, *Int. J. Biol. Macromol.*, 2022, **222**, 2843–2854.
- 52 A. Adjali, A. R. N. Pontillo, E. Kavetsou, A. Katopodi, A. Tzani, S. Grigorakis, S. Loupassaki and A. Detsi, Clove Essential Oil-Hydroxypropyl- $\beta$ -Cyclodextrin Inclusion Complexes: Preparation, Characterization and Incorporation in Biodegradable Chitosan Films, *Micro*, 2022, **2**, 212–224.
- 53 H. Liu, Z. Zhao, W. Xu, M. Cheng, Y. Chen, M. Xun, Q. Liu and W. Wang, Preparation, Characterization, Release and Antibacterial Properties of Cinnamon Essential Oil Microcapsules, *Coatings*, 2023, **13**(6), DOI: [10.3390/coatings13060973](https://doi.org/10.3390/coatings13060973).
- 54 P. Çoruhlu, A. R. Ergün and T. Baysal, Characterization of chitosan films incorporating thyme oil and its effect on black olives, *Ital. J. Food Sci.*, 2025, **37**, 307–318.
- 55 A. Halloub, M. Raji, H. Essabir, S. Nekhlaoui, M. O. Bensalah, R. Bouhfid and A. el kacem Qaiss, Stable smart packaging betalain-based from red prickly pear covalently linked into cellulose/alginate blend films, *Int. J. Biol. Macromol.*, 2023, **234**, 123764.
- 56 S. Bhatia, Y. Abbas Shah, A. Al-Harrasi, M. Jawad, E. Koca and L. Y. Aydemir, Enhancing Tensile Strength, Thermal Stability, and Antioxidant Characteristics of Transparent Kappa Carrageenan Films Using Grapefruit Essential Oil for Food Packaging Applications, *ACS Omega*, 2024, **9**, 9003–9012.
- 57 A. Ghosh and M. A. Ali, Studies on physicochemical characteristics of chitosan derivatives with dicarboxylic acids, *J. Mater. Sci.*, 2012, **47**, 1196–1204.
- 58 K. Ram and A. Harit, Physico-chemical properties of lignin – alginate based films in the presence of different plasticizers, *Iran. Polym. J.*, 2016, **25**, 661–670.



- 59 J. F. Silva, C. T. Guedes, E. da Silva Alves, B. H. F. Saqueti, C. S. R. Ferreira, A. P. M. de Mendonça, M. W. C. Silva, F. Sato, B. A. de Abreu Filho, O. de Oliveira Santos Júnior, S. C. da Costa, S. S. dos Santos, M. R. da Silva Scapim and G. S. Madrona, Active biodegradable films based on gelatin/alginate incorporated with microencapsulated Mamacadela extract: Antioxidant, antibacterial, and UV-barrier properties, *Food Res. Int.*, 2026, **231**, 118712.
- 60 S. Mariño-Cortegoso, A. Lestido-Cardama, R. Sendón, A. R. B. de Quirós and L. Barbosa-Pereira, The State of the Art and Innovations in Active and Edible Coatings and Films for Functional Food Applications, *Polymers*, 2025, **17**, DOI: [10.3390/POLYM17182472](https://doi.org/10.3390/POLYM17182472).
- 61 S. Ebrahimzadeh, M. Rezazadeh, H. Hamishehkar, S. Kafil and L. Lim, Essential oils-loaded electrospun chitosan-poly ( vinyl alcohol ) nonwovens laminated on chitosan film as bilayer bioactive edible films, *LWT*, 2021, **144**, 111217.
- 62 E. M. Zadeh, S. F. O. Keefe and Y. Kim, Utilization of Lignin in Biopolymeric Packaging Films, *ACS Omega*, 2018, **3**, 7388–7398.
- 63 A. Dghoughi, M. Raji and A. el kacem Qaiss, Synthesis and sustainable applicability of triangular lignin nanoparticles in sunscreen formulations and UV shielding', *New J. Chem.*, 2025, **49**, 9145–9156.
- 64 R. Kamal, M. Kharbach, J. D. Imig, M. Eljmeli, Z. Doukkali, H. N. Mrabti, H. Elmsellem, A. Bouklouze, Y. Cherrah and K. Alaoui, Antioxidant Activities, Total Polyphenolic Compounds and HPLC/DAD/MS Phenolic Profile of Argan Oil Derived from Two Different Methods of Extractions, *J. Mater. Environ. Sci.*, 2017, **8**, 1320–1327.
- 65 C. Rachida, M. Khadija, A. Fadila and S. Abdelaziz, Protective and antioxidant potential of the argan oil on induced oxidative stress in *Tetrahymena pyriformis*, *J. Med. Plants Res.*, 2013, **7**, 1961–1968.
- 66 C. Ibarra-Alvarado, A. Rojas, S. Mendoza, M. Bah, D. M. Gutiérrez, L. Hernández-Sandoval and M. Martínez, Vasoactive and antioxidant activities of plants used in Mexican traditional medicine for the treatment of cardiovascular diseases, *Pharm. Biol.*, 2010, **48**, 732–739.
- 67 H. Amzal, K. Alaoui, S. Tok, A. Errachidi, R. Charof, Y. Cherrah and A. Benjouad, Protective effect of saponins from *Argania spinosa* against free radical-induced oxidative haemolysis, *Fitoterapia*, 2008, **79**, 337–344.
- 68 S. Shao-Ni, C. Xue-Fei, X. Feng, L. J. Gwynn and B. Mark, Alkaline and Organosolv Lignins from Furfural Residue: Structural Features and Antioxidant Activity, *Bioresources*, 2013, **9**, 772–785.
- 69 J. Csapó, J. Prokisch, Cs. Albert and P. Sipos, Effect of UV light on food quality and safety, *Acta Univ. Sapientiae, Aliment.*, 2019, **12**, 21–41.
- 70 A. Dghoughi, F. Nazih, A. Halloub and M. Raji, International Journal of Development of shelf life-extending packaging for vitamin C syrup based on high-density polyethylene and extracted lignin argan shells, *Int. J. Biol. Macromol.*, 2023, **242**, 125077.
- 71 H. Sadeghifar and A. Ragauskas, Lignin as a UV Light Blocker—A Review, *Polymers*, 2020, **12**, 1134.
- 72 S. Tanpichai, K. Yuwawech, E. Wimolmala, Y. Srimarut, W. Woraprayote and Y. Malila, Enhanced physical, mechanical and barrier properties of chitosan films via tannic acid cross-linking, *RSC Adv.*, 2025, **15**, 30742–30757.
- 73 R. M. Vieira, E. Gauthier, G. Widanagamage, N. McKenzie, K. Dunn, L. Moghaddam, P. Halley and M. Brienzo, UV-blocking and hydrophobicity improvement of chitosan-based film with lignin addition from a pilot scale-up Organosolv process of Banana Pseudostem, *Int. J. Biol. Macromol.*, 2025, **313**, 144254.
- 74 J. Chen, J. Tian, S. Zhang, A. Nilghaz, Y. Xie and X. Wan, Balance of Lignin Light-Color and UV-Shielding Properties: Pyruvic Acid Fractionation for Green Sunscreen Formulations, *ACS Sustain. Chem. Eng.*, 2023, **11**, 17806–17815.
- 75 Y. Dong, J. Deng and X. Yan, Preparation of Tung Oil Microcapsules Coated with Chitosan Sodium Tripolyphosphate and Their Effects on Coating Film Properties, *Coatings*, 2025, **15**, DOI: [10.3390/coatings15080867](https://doi.org/10.3390/coatings15080867).
- 76 J. Hang, Y. Han, X. Yan and J. Li, Effect of Shellac-Rosin Microcapsules on the Self-Healing Properties of Waterborne Primer on Wood Surfaces, *Coatings*, 2025, **15**, DOI: [10.3390/coatings15091003](https://doi.org/10.3390/coatings15091003).
- 77 T. Dobashi, T. Narita, J. Masuda, K. Makino, T. Mogi, H. Ohshima, M. Takenaka and B. Chu, Light Scattering of a Single Microcapsule with a Hydrogel Membrane, *Langmuir*, 1998, **14**, 745–749.
- 78 ISO 22196:2011 - Measurement of antibacterial activity on plastics and other non-porous surfaces, <https://www.iso.org/standard/54431.html>, accessed 31 March 2026.
- 79 I. F. Sulistiyani and A. T. Prasetya, Antibacterial Activity of Cajuputi Oil (*Melaleuca leucadendron*) Microcapsules Against *Staphylococcus aureus* Bacteria Applied to Cotton Fabric Fibers, *Indones. J. Chem. Sci.*, 2022, **11**, DOI: [10.15294/jjcs.v11i1.53445](https://doi.org/10.15294/jjcs.v11i1.53445).
- 80 F. Z. Semlali Aouragh Hassani, K. El Bourakadi, N. Merghoub, A. el kacem Qaiss and R. Bouhfid, Effect of chitosan/modified montmorillonite coating on the antibacterial and mechanical properties of date palm fiber trays, *Int. J. Biol. Macromol.*, 2020, **148**, 316–323.
- 81 A. C. Duarte, L. Fernández, A. Jurado, A. B. Campelo, Y. Shen, A. Rodríguez and P. García, Synergistic removal of *Staphylococcus aureus* biofilms by using a combination of phage Kayvirus rodi with the exopolysaccharide depolymerase Dpo7, *Front. Microbiol.*, 2024, **15**, 1438022.
- 82 L. Yuan, W. Feng, Z. Zhang, Y. Peng, Y. Xiao and J. Chen, Effect of potato starch-based antibacterial composite films with thyme oil microemulsion or microcapsule on shelf life of chilled meat, *LWT*, 2021, **139**, DOI: [10.1016/j.lwt.2020.110462](https://doi.org/10.1016/j.lwt.2020.110462).
- 83 M. D. A. S. das Neves, S. Scandorieiro, G. N. Pereira, J. M. Ribeiro, A. B. Seabra, A. P. Dias, F. Yamashita, C. B. D. O. S. R. Martinez, R. K. T. Kobayashi and G. Nakazato, Antibacterial Activity of Biodegradable Films



- Incorporated with Biologically-Synthesized Silver Nanoparticles and the Evaluation of Their Migration to Chicken Meat, *Antibiotics*, 2023, **12**, 1, DOI: [10.3390/antibiotics12010178](https://doi.org/10.3390/antibiotics12010178).
- 84 X. Zhang, Z. Zhang, W. Wu, J. Yang and Q. Yang, Preparation and characterization of chitosan/Nano-ZnO composite film with antimicrobial activity, *Bioprocess Biosyst. Eng.*, 2021, **44**, 1193–1199.
- 85 A. S. Abreu, M. Oliveira, A. De Sá, R. M. Rodrigues, M. A. Cerqueira, A. A. Vicente and A. V. Machado, Antimicrobial nanostructured starch based films for packaging, *Carbohydr. Polym.*, 2015, **129**, 127–134.
- 86 N. Durán, G. Nakazato and A. B. Seabra, Antimicrobial activity of biogenic silver nanoparticles, and silver chloride nanoparticles: an overview and comments, *Appl. Microbiol. Biotechnol.*, 2016, **100**, 6555–6570.
- 87 M. N. Collins and M. Culebras, Letter from the Editors: Sustainable Biopolymers and Composites for Biomedical Applications, in *Sustainable Biopolymers and Composites for Biomedical Applications*, ed. M. N. Collins and M. Culebras, Biomaterials, Bioengineering and Sustainability, Springer, Cham, 2025, vol 5, DOI: [10.1007/978-3-031-91972-5\\_1](https://doi.org/10.1007/978-3-031-91972-5_1).
- 88 J. K. Patra and K. H. Baek, Antibacterial activity and synergistic antibacterial potential of biosynthesized silver nanoparticles against foodborne pathogenic bacteria along with its anticandidal and antioxidant effects, *Front. Microbiol.*, 2017, **8**, 227226.
- 89 S. Rawdkuen, Edible Films Incorporated with Active Compounds: Their Properties and Application, in *Active Antimicrobial Food Packaging*, 2019, DOI: [10.5772/intechopen.80707](https://doi.org/10.5772/intechopen.80707).
- 90 M. Pateiro, M. Gagaoua, F. J. Barba, W. Zhang and J. M. Lorenzo, A Comprehensive Review on Lipid Oxidation in Meat and Meat Products, *Antioxidants*, 2019, **8**, 1–31.
- 91 C. A. Daley, A. Abbott, P. S. Doyle, G. A. Nader and S. Larson, A review of fatty acid profiles and antioxidant content in grass-fed and grain-fed beef, *Nutr. J.*, 2010, **9**, 1–12.
- 92 B. Sun, F. Xu, D. Chen and J. Liu, Quaternary ammonium chitosan-based active packaging films incorporated with dialdehyde guar gum-proanthocyanidins conjugates: characterization and application in the edible coating of pork, *Food Hydrocoll.*, 2025, **158**, 110597.
- 93 V. Pavoncello, F. Barras and E. Bouveret, Degradation of Exogenous Fatty Acids in Escherichia coli, MDPI, 2022, DOI: [10.3390/biom12081019](https://doi.org/10.3390/biom12081019).
- 94 X. Luo, Y. Peng, Z. Qin, W. Tang, G. J. Duns, W. Dessie, N. He and Y. Tan, Chitosan-based packaging films with an integrated antimicrobial peptide: characterization, in vitro release and application to fresh pork preservation, *Int. J. Biol. Macromol.*, 2023, **231**, 123209.
- 95 G. Manassis, A. I. Kalogianni, T. Lazou and M. Moschovas, Plant-Derived Natural Antioxidants in Meat and Meat Products, *Antioxidants*, 2020, **9**, 1215.
- 96 P. Cazón, A. Antoniewska, J. Rutkowska and M. Vázquez, Evaluation of easy-removing antioxidant films of chitosan with Melaleuca alternifolia essential oil, *Int. J. Biol. Macromol.*, 2021, **186**, 365–376.
- 97 T. A. Nguyen, Characterization of Chitosan-Based Active Film Incorporating with Gallic Acid, *Int. J. Multidiscipl. Res. Anal.*, 2023, DOI: [10.47191/ijmra/v6-i8-40](https://doi.org/10.47191/ijmra/v6-i8-40).
- 98 X. Liu, F. Xu, H. Yong, D. Chen, C. Tang, J. Kan and J. Liu, Recent advances in chitosan-based active and intelligent packaging films incorporated with flavonoids, *Food Chem.: X*, 2025, **25**, 102200.
- 99 A. A. Dera, I. Ahmad, P. Rajagopalan, M. Al Shahrani, A. Saif, M. Y. Alshahrani, Y. Alraey, A. M. Alamri, S. Alasmari, M. Makkawi, A. G. Alkhathami, G. Zaman, A. Hakami, R. Alhefzi and M. A. Alfhili, Synergistic efficacies of thymoquinone and standard antibiotics against multi-drug resistant isolates, *Saudi Med. J.*, 2021, **42**, 196–204.
- 100 S. R. Kanatt, M. S. Rao, S. P. Chawla and A. Sharma, Effects of chitosan coating on shelf-life of ready-to-cook meat products during chilled storage, *LWT-Food Sci. Technol.*, 2013, **53**, 321–326.

